RESEARCH ARTICLE

WILEY

Effects of riverbed incision on the hydrology of the Vietnamese Mekong Delta

Doan Van Binh[1,2] ⓘ | Sameh A. Kantoush[1] ⓘ | Tetsuya Sumi[1] ⓘ |
Nguyen Phuong Mai[3] | Trieu Anh Ngoc[2] ⓘ | La Vinh Trung[4] | Tran Dang An[2] ⓘ

[1]Water Resources Research Center, Disaster Prevention Research Institute, Kyoto University, Uji-shi, Japan

[2]Department of Water Resources Engineering, Thuyloi University, Hanoi, Vietnam

[3]Department of Civil Engineering, Thuyloi University, Hanoi, Vietnam

[4]Research Management Department, Vietnamese-German University, Thủ Dầu Một, Vietnam

Correspondence
Doan Van Binh, Water Resources Research Center, Disaster Prevention Research Institute, Kyoto University, Goka-sho, Uji-shi, 611-0011, Japan.
Email: doan.binhvan.3e@kyoto-u.ac.jp; binhdv@tlu.edu.vn

Abstract

The hydrogeomorphology of the Vietnamese Mekong Delta (VMD) has been significantly altered by natural and anthropogenic drivers. In this study, the spatiotemporal changes of the flow regime were examined by analysing the long-term daily, monthly, annual and extreme discharges and water levels from 1980 to 2018, supported by further investigation of the long-term annual sediment load (from the 1960s to 2015), river bathymetric data (in 1998, 2014 and 2017) and daily salinity concentration (from the 1990s to 2015) using various statistical methods and a coupled numerical model. Then, the effects of riverbed incision on the hydrology were investigated. The results show that the dry season discharge (i.e., in March–June) of the Tien River increased by up to 23% from the predam period (1980–1992) to the postdam period (1993–2018) but that the dry season water level at My Thuan decreased by up to −46%. The annual mean and monthly water levels in June at Tan Chau and in January and June–October at My Thuan in the Tien River decreased statistically, even though the respective discharges increased significantly. These decreased water levels instead of the increased discharges were attributed to the accelerated riverbed incision upstream from My Thuan, which increased by more than three times, from a mean rate of −0.16 m/year (−16.7 Mm^3/year) in 1998–2014 to −0.5 m/year (−52.5 Mm^3/year) in 2014–2017. This accelerated riverbed incision was likely caused by the reduction in the sediment load of the VMD (from 166.7 Mt/year in the predam period to 57.6 Mt/year in the postdam period) and increase in sand mining (from 3.9 Mm^3 in 2012 to 13.43 Mm^3 in 2018). Collectively, the decreased dry season water level in the Tien River is likely one of the main causes of the enhanced salinity intrusion.

KEYWORDS
dam, discharge, flow regime, riverbed incision, salinity intrusion, sand mining, Vietnamese Mekong Delta, water level

1 | INTRODUCTION

The Vietnamese Mekong Delta (VMD) is one of the most important deltas in the world in terms of rice production and fisheries (Binh, Kantoush, Mai, & Sumi, 2018; Manh et al., 2014). It is home to around 17 million people whose livelihoods depend largely on agro-aquaculture, which contributes 18% of the GDP in Vietnam (Tran et al., 2019). This high productivity results from natural flood pulses that transport large amounts of nutrient-rich suspended sediment (43–167 Mt/year) and provide plenty of fish from the Mekong River (or simply Mekong) to the delta (Binh et al., 2020; Kondolf et al., 2014; Manh et al., 2014, 2015). However, the sustainable development of the VMD is challenged by various environmental pressures, including riverbed incision, riverbank and coastal erosion, flow regime alterations, fertile sediment reduction and salinity intrusion (Anthony et al., 2015; Binh, Kantoush, Sumi, & Mai, 2018; Chapman & Darby, 2016; Eslami et al., 2019; Kummu et al., 2008; D. Li et al., 2017; Park et al., 2020; Tran et al., 2019).

Flow regime and morphological changes are critical issues for rivers worldwide (e.g., Batalla et al., 2004; Bizzi et al., 2015; Fitzhugh & Vogel, 2011; Ijaz et al., 2020; Yu et al., 2013; Zhang et al., 2014). Likewise, the pristine hydro-geomorphology of the Mekong has been significantly altered, largely due to dams, climate change, sea level rise, land use change and dyke systems (Arias et al., 2014; Binh et al., 2020; Binh et al 2018; Brunier et al., 2014; Dang et al., 2016; Eslami et al., 2019; Hackney et al., 2020; Hoa et al., 2007; Hoang et al., 2016, 2019; Lauri et al., 2012; D. Li et al., 2017; Lu, Li, et al., 2014; Triet et al., 2017; Xue et al., 2011). Although there is uncertainty in climate projections (Lauri et al., 2012; Manh et al., 2015), climate change/variability has been reported to reduce the sediment load (Darby et al., 2016) and to enhance the magnitude and frequency of extreme events (Hoang et al., 2016; Hoanh et al., 2010). Dyke systems have been revealed to shift the floods in protected areas to unprotected areas and to have negative impacts on ecosystem services and agricultural production (Dang et al., 2016; Tran et al., 2018, 2019; Triet et al., 2017), whereas irrigation expansion is likely to reduce the annual flow (Hoang et al., 2019). Dams have significantly altered the seasonal flows of the Mekong by reducing the flood flows and increasing the dry flows (Hoang et al., 2019; D. Li et al., 2017; Lu, Li, et al., 2014; Räsänen et al., 2017). Dams have also trapped large volumes of sediment in reservoirs, resulting in reduced sediment load and increased riverbed incision downstream (Besset et al., 2019; Best, 2019; Binh et al., 2020; Kondolf et al., 2014; Kummu et al., 2008; Kummu et al., 2010; Kummu & Varis, 2007; Lu & Siew, 2006). Riverbed incision has also been caused by large-scale sand mining (Brunier et al., 2014; Eslami et al., 2019; Hackney et al., 2020; Jordan et al., 2019). Bravard et al. (2013) reported a mined volume of sand of over 31 Mm^3 along the Mekong mainstem in 2011–2012. In turn, riverbed incision has been attributed to enhanced salinity intrusion, along with tidal amplification caused by sea level rise and dams (Eslami et al., 2019; Mai et al., 2018). The mesotidal regime in the river mouth area strongly influences the flow regime and salinity intrusion during the dry season in the VMD,

peaking in March and April; however, the tidal signal is limited up-river during the flood season when fluvial processes can have effects up to 100 km seaward of the river mouth (Gugliotta et al., 2017).

The existing studies have provided useful insights into the effects of anthropogenic activities and climate change/variability on the flow regime, suspended sediment load, morphological changes and salinity intrusion in the Mekong basin. However, the effects of riverbed incision on hydrological processes are poorly understood because of the complex interactions among the fluvial flows and tidal regimes. Recently, Binh et al. (2020) examined the effects of upstream dams on the discharges, sediment loads and morphological changes in the VMD. They found that upstream dams have small effects on the annual daily mean discharge, although these dams are the main causes of sediment reduction and riverbed incision. However, in this study, riverbed incision was only quantified in the period of the development of post-mega-dams (reservoir capacity >10^9 m^3, e.g., Nuozhadu and Xiaowan) between 2014 and 2017, whereas the effects of the development of pre-mega-dams on riverbed incision were not adequately assessed. Moreover, water levels were not analysed because the effect of riverbed incision on the hydrology was not the focus of these studies. Although the subtidal (at Tan Chau and Chau Doc) and non-tidal (at Kratie) discharges in the dry season have recently increased, substantial increases in salinity intrusion were also observed in the VMD (Eslami et al., 2019). This finding indicates that changing water level patterns and recently observed extreme seawater intrusion in the VMD may depend not only on upstream discharge and tidal regimes, but also on riverbed incision. However, the relationship between riverbed incision and water level changes is poorly understood, especially in the context of changing upstream discharge and sediment load before and after the operation of upstream dams, coupled with intensive sand mining activities in the VMD. Therefore, it is necessary to examine the effects of riverbed incision on reducing the riverine water level, which is likely one of the main causes of accelerated salinity intrusion. Insights into the effects of riverbed incision on water levels may facilitate the development of sustainable water resource management plans in the global deltas. With this regard, the objectives of this study were (1) to examine the spatiotemporal alterations of the long-term discharge and water level in the VMD in terms of magnitude, timing, duration and frequency and (2) to relate flow regime alterations (i.e., water level reduction) to riverbed incision caused by dam-induced decreases in sediment load and sand mining, supported by a hydro-sediment-morpho dynamics model. We then examined some implications of the riverbed incision-induced water level reduction on the increased salinity intrusion in the delta, besides the tidal amplification and riverbed incision-induced tidal velocity increase addressed by Eslami et al. (2019).

The remainder of this paper is organized as follows. Sections 2 and 3 thoroughly describe the study area, including the flow regime characteristics identified previously and the data acquisition methods and analysis techniques employed in the present study, respectively. Sections 4 and 5 respectively provide a detailed presentation of the measurement and analysis results and their significance in the context of the research objectives. Section 6 discusses possible uncertainties
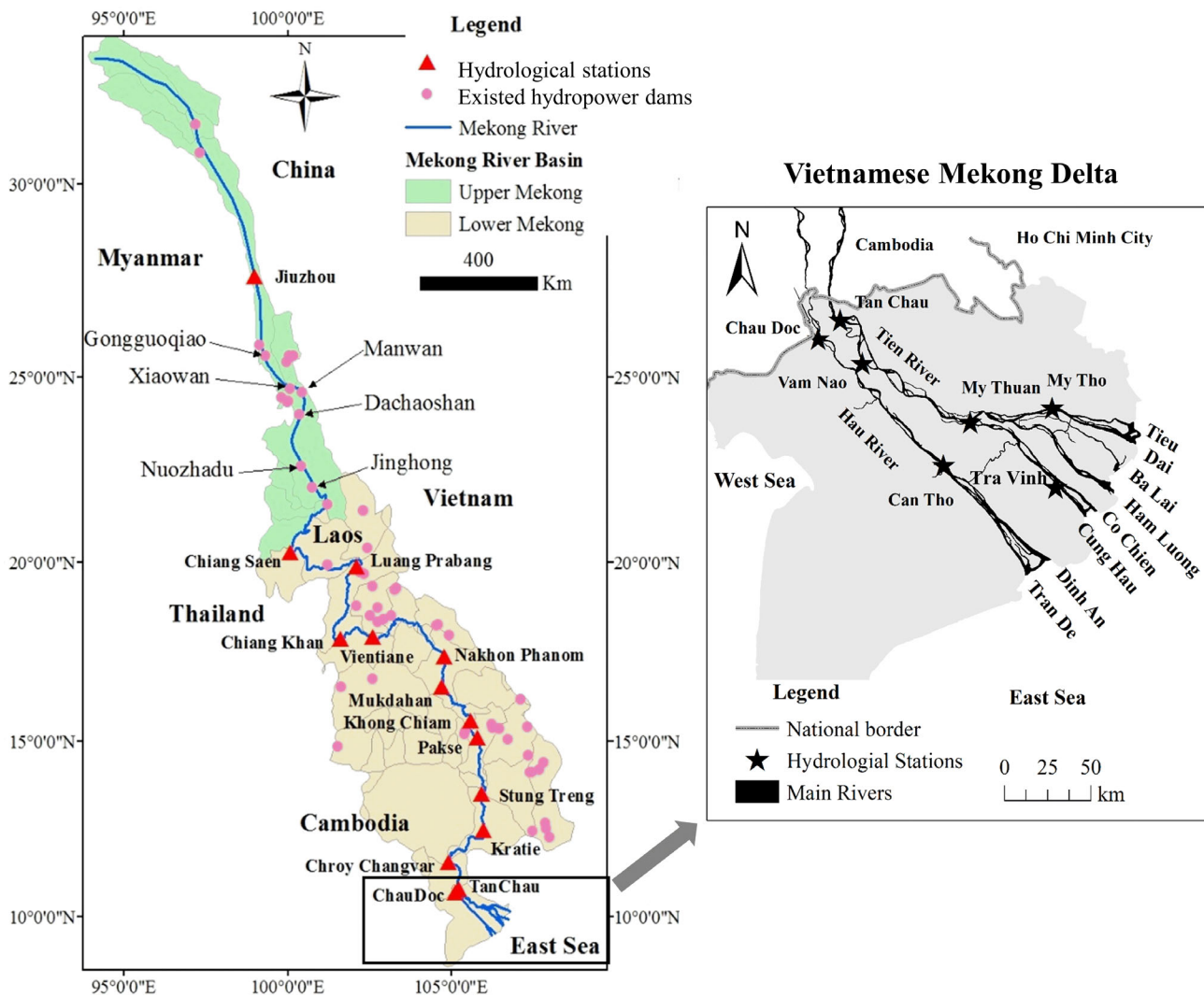
FIGURE 1 Spatial coverage of the Mekong basin and VMD: Locations of dams and hydrological stations. Tan Chau and Chau Doc are the uppermost hydrological stations in the VMD

of the present study. Finally, Section 7 clearly highlights the main contributions of this study and scope for future research.

2 | STUDY AREA

The VMD lies in the lowermost part of the Mekong, which flows through China, Myanmar, Laos, Thailand, Cambodia and Vietnam. Its total area is approximately 39 000 km^2, stretching from the Vietnam–Cambodia border to the East and West Seas of Vietnam (Figure 1). The Tien and Hau Rivers (the Vietnamese names of the Mekong and Bassac Rivers, respectively) are the two main distributaries, having lengths of approximately 250 and 220 km, respectively (Kantoush et al., 2017). These rivers discharge water into the sea via eight branches through a complex channel network and spacious floodplains, which have an average ground elevation of 0.7–1.2 m.

Large dams (>15 m high) have been increasingly built and planned in the Mekong basin since the 1990s under the pressure of population

expansion and economic growth. Sixty-four dams (Figure 1) had been completed in this area by 2015 (Kondolf et al., 2014) with a total storage capacity of over 80 km^3, accounting for more than 96% and 20% of the annual discharges at Chiang Saen and Kratie, respectively. Further, six mega-dams (reservoir capacity >10^9 m^3) in the Lancang cascade contribute more than 51% (41.2 km^3) of the total storage capacity of all 64 dams (Table 1). Manwan was the first in operation in 1993. Sand mining is another stressor on water-related management in the Mekong. In the VMD, sand has been increasingly mined from the riverbed, from 7.75 Mm^3 in 2012 to 29.3 Mm^3 (including 4.6 Mm^3 from dredging) in 2018 (Bravard et al., 2013; Jordan et al., 2019). The mined sand is mainly used for land reclamation, export and concrete production and construction to fuel economic development in Vietnam, especially in Ho Chi Minh City.

The flow regime of the delta is hydrologically characterized by two distinct seasons: the flood season, mainly triggered by Asian monsoons and tropical cyclones, usually starts in June/July and ends in November/December and the dry season lasts for the other

TABLE 1 Profiles of major commissioned dams in the Mekong basin

Name	Geomorphic region	Catchment area (km^2)	Annual inflow (m^3/s)	Dam height (m)	Active storage (km^3)	Total storage (km^3)	Annual generation (GWh)	Reservoir filling year
Nuozhadu	Lancang	144 700	1750	260	12.2	22.37	23 780	2011
Xiaowan	Lancang	113 300	1220	292	9.9	15.13	18 890	2008
Jinghong	Lancang	149 100	1840	107	0.25	1.23	8060	2008
Manwan	Lancang	114 500	1230	132	0.26	1.06	7810	1993
Daochaoshan	Lancang	121 000	1340	120.5	0.37	0.88	6700	2001
Gongguoqiao	Lancang	97 300	985	130	0.12	0.51	4060	2011
Nam Tha 1	Pull Apart	8990	186	-	0.68	0.95	-	2015
Nam Khan 2	Loei Fold	5221	63	-	0.53	1.22	-	2015
Nam Poun	Loei Fold	1700	89	-	0.34	0.47	-	2015
Nam Lik 2	Loei Fold	1993	98	-	0.83	1.34	-	2010
Nam Ngum 2	Loei Fold	5640	193	-	2.99	3.59	-	2011
Nam Theun 2	Annamite Mountains	4013	244	-	3.38	3.68	-	2010
Xe Kong 3up	Kon Tum Massif	5882	241	-	0.10	0.43	-	2012
Plei Krong	Kon Tum Massif	3216	127	-	0.95	1.05	-	2009
Yali	Kon Tum Massif	7455	263	-	0.78	1.04	-	2001
Buon Tua Srah	Tertiary Volcanic Plateau	2930	102	-	0.52	0.79	-	2009

Note: Sources: (Fan et al. (2015); Kondolf et al. (2014); J. Li et al. (2012).

half of the year (Figure S1). The dry season is characterized by salinity intrusion from the sea. The intrusion length of saline water reaches 60–70 km in extreme drought years, for example, the drought event in 2015–2016 (Kantoush et al., 2017). The discharge of the Tien River is approximately four times that of the Hau River. The mean discharges (based on the 1980–2018 data used in this study) at Tan Chau and Chau Doc are 10 009 and 2475 m^3/s, respectively, resulting in two distinct stages: the rising stage (April–September) and falling stage (October–March of the following year) (Figure S1).

3 | DATA AND METHODS

3.1 | Flow, sediment and salinity data

We analysed time series of daily, monthly, seasonal, annual and extreme discharges and water levels at Tan Chau, Chau Doc, My Thuan and Can Tho (Figure 1) for the period of 1980–2018 to elucidate the long-term flow regime alterations in the VMD. Although these four key stations have long-term monitored discharge and water level data, the spatiotemporal differences in the flow patterns enable identification of the driving factors. The analyses were performed based on the daily discharge and water level data, which

were the averages of the hourly data provided by the Vietnamese National Hydro-Meteorological Data Centre. The daily discharge and water level data are equivalent to the data de-tided using a 25 h moving average filter (Foreman et al., 1995). The trends in the de-tided discharge and water level data were considered in this study because the trends in the tidal data were previously analysed by Eslami et al. (2019). Hourly subtidal water level data at Tan Chau, Chau Doc, My Thuan and Can Tho were collected from 1980 to 2018. From 1996, hourly subtidal discharge data were available, but only daily discharge data were available some months of the year in both the flood and dry seasons between 1980 and 1995. By developing rating curves, the gaps in the data were filled. Figure S2 shows that the discharge and water level have a clockwise hysteresis relation with the rising stage from April to September and the falling stage from October to March. Therefore, the rating curves at Tan Chau and Chau Doc were established for these two stages separately by using all available daily data at each station. The rating equations were established using polynomial regression analysis with the least squares method. The equations corresponding to the rising and falling stages at Tan Chau are shown in Equations (1) and (2), respectively and those at Chau Doc are presented in Equations (3) and (4), respectively:

$$Q = -913H^2 + 9243H - 1060.7, \tag{1}$$
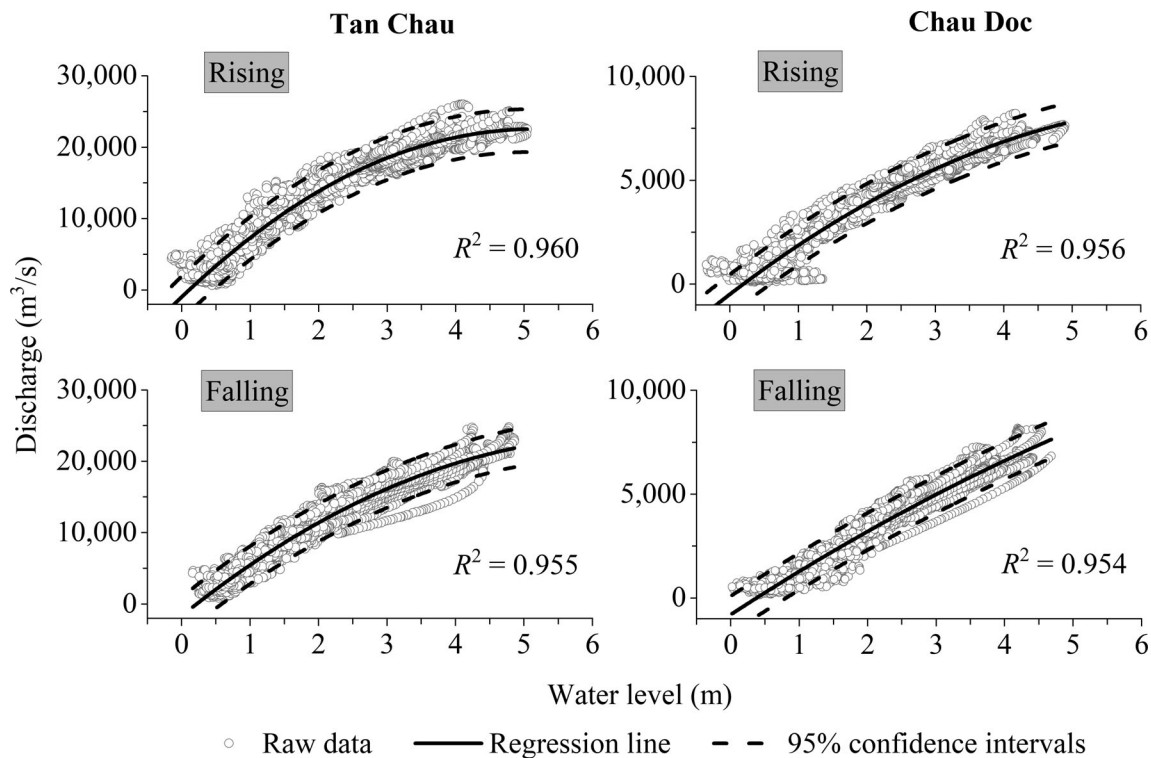
FIGURE 2 Stage-discharge rating curves at Tan Chau and Chau Doc in the rising and falling stages

$$Q = -592H^2 + 7711H - 1643.7, \qquad (2)$$

$$Q = -174H^2 + 2532H - 484.5, \qquad (3)$$

$$Q = -75H^2 + 2153H - 796.9, \qquad (4)$$

where Q (dependent variable) is the discharge (m^3/s) and H (independent variable) is the water level (m). The established rating equations yielded high coefficients of determination, $R^2 > 0.95$ (Figure 2). Moreover, most of the values fall within the 95% confidence interval, indicating strong agreement between the measured and predicted discharges. Notably, some discharge values were under- or over-estimated in the extreme drought (2015) or flood (2000) years. Therefore, the regression coefficients in these rating curves will need to be updated when new data from the coming years become available in future studies.

We additionally analysed the daily discharge at Chiang Saen, Mukdahan and Kratie along the lower Mekong for the period of 1960–2015 (data from the Mekong River Commission) and the annual rainfall at seven stations in the Mekong basin, including Licang, Simao, Lancang and Jinghong (in China); Chiang Saen and Nong Khai (in Thailand); and Pakse (in Laos), for the period of 1950–2016. The changes in the sediment loads at Chiang Saen, Luang Prabang, Nong Khai (close to Vientiane), Mukdahan, Khong Chiam, Tan Chau and Chau Doc from the 1960s to 2015 were also investigated. Annual sediment loads were available at Chiang Saen, Luang Prabang, Nong Khai, Mukdahan and Khong Chiam which were well estimated by

Lu & Siew, 2006; Wang et al., 2011; Koehnken, 2014; Lu, Kummu, & Oeurng, 2014. At Tan Chau and Chau Doc, daily suspended sediment concentrations (SSCs) were available in 1993–2015. In 1980–1992, daily SSCs were available in several months a year at Tan Chau, whereas Chau Doc did not have any record. Therefore, the missing daily SSCs at Tan Chau in 1980–1992 were estimated by the daily SSC-discharge rating curves established for the rising and falling stages separately. Then, the multiplication of the daily SSCs at Tan Chau with a factor of 13.3% (the mean ratio of the suspended sediment loads between Chau Doc and Tan Chau in 1993–2015) yielded the corresponding daily SSCs at Chau Doc. The daily suspended sediment loads were then estimated as the products of daily SSCs and the respective daily discharges. The details of the data sources and treatment of the sediment load data were described by Binh et al. (2020). Moreover, the daily salinity concentrations at stations near the estuaries of the VMD from the 1990s to 2018 were analysed. The locations and data ranges of the analysed stations are shown in Figure 1 and Table 2, respectively.

3.2 | Bathymetric field measurements and data processing

We conducted boat-based bathymetric measurements along approximately 570 km of the Tien and Hau Rivers and the Vam Nao channel in August–September 2017. The measured extent was from Tan Chau/ Chau Doc to the river mouths (i.e., Co Chien, Cung Hau, Dinh An and Tran De distributaries) (Figure 1). A Teledyne RD Instruments Work-

TABLE 2 Long-term water level, discharge, sediment load, salinity concentration and precipitation data in the Mekong basin used in this study

Station	Country	Water level	Discharge	Sediment	Salinity	Precipitation
Lincang	China	-	-	-	-	1954–2014
Simao	China	-	-	-	-	1954–2014
Lancang	China	-	-	-	-	1954–2014
Jinghong	China	-	-	-	-	1954–2014
Chiang Saen	Thailand	-	1960–2014	1961–2013	-	1966–2016
Luang Prabang	Laos	-	-	1961–2013	-	-
Nong Khai	Thailand	-	-	1961–2013	-	1973–2016
Mukdahan	Thailand	-	1960–2012	1961–2013	-	-
Khong Chiam	Thailand	-	-	1962–2013	-	-
Pakse	Laos	-	-	-	-	1950–2016
Kratie	Cambodia	-	1960–2015	-	-	-
Tan Chau	Vietnam	1980–2018	1980–2018	1980–2015	-	-
Chau Doc	Vietnam	1980–2018	1980–2018	1980–2015	-	-
My Thuan	Vietnam	1980–2018	-	-	-	-
Can Tho	Vietnam	1980–2018	-	-	-	-
An Thuan	Vietnam	-	-	-	1990–2018	-
Binh Dai	Vietnam	-	-	-	1997–2018	-

Note: The locations of the stations are shown in Figure 1.

horse Rio Grande 600 kHz acoustic Doppler current profiler (ADCP) equipped with a Trimble GPS was used to measure the river depths of 200 cross-sections. The ADCP was mounted 0.3 m below the water surface and the distance between cross-sections was 1–5 km. We also collected hourly water level data at 11 hydrological stations (provided by the Vietnamese National Hydro-Meteorological Data Centre) along these rivers during the survey period. The raw river depth data were filtered by high- and low-pass filters and then processed using the Teledyne RD Instrument WinRiver II software. Meanwhile, we interpolated the hourly water level data in a matrix of distance and time to the measured cross-sections. Eventually, the riverbed elevations were obtained by subtracting the water levels from the corresponding river depths.

In evaluating the morphological changes, the riverbed elevations in 1998 and 2014 were also collected from Thuyloi University and the Southern Institute of Water Resources Research, Vietnam. The 1998 bathymetric data originally distributed by the Mekong River Commission were measured by a bi-frequency echosounder (Brunier et al., 2014) in all of the main rivers in the VMD with a distance between cross-sections of 300–500 m. The 2014 bathymetric data, measured by the ADCP, consisted of 491 cross-sections in the upper Tien River (from Tan Chau to My Thuan) and the Vam Nao channel with a distance between cross-sections of 200–1000 m. All bathymetric datasets from 1998, 2014 and 2017 were in *xyz* coordinates (point data) which were projected to WGS 1984 Universal Transverse Mercator, zone 48 N using the national datum of Vietnam at Ha Tien (Gulf of Thailand).

Our objective was to assess the morphological changes in the upper Tien River and Vam Nao channel because of the availability of the 2014 dataset. For this purpose, the bathymetric point data were interpolated and converted into raster mode using *ArcGIS®10*. We used isotropic universal Kriging accompanied by the exponential method with the kernel function to interpolate the point data, as this choice was the best in 111 trials performed using the deterministic and geostatistical methods available in the *Geostatistical Analyst* module in *ArcGIS®10*. The interpolated riverbed elevation maps in all considered years had the same spatial resolution of 40 m. Finally, we estimated the morphological changes in depth (m) and volume (m^3) from 1998 to 2014 and from 2014 to 2017 by subtracting the riverbed elevations in the two considered years using the Geomorphic Change Detection (*GCD®6*) add-in in *ArcGIS®10*. To eliminate the errors arising from the instruments themselves and from employing different instruments in different years, differences in riverbed elevation between the two datasets from −0.6 to +0.6 m were excluded from the comparison (Brunier et al., 2014). The field survey, data acquisition, data processing and data comparison methods were described in greater detail by Binh et al. (2020). Because the numbers of years from 1998 to 2014 and from 2014 to 2017 were different, the mean annual riverbed incision/deposition maps in the two periods were generated and compared. This quantitative comparison was the additional contribution from this study compared to Binh et al. (2020), in which the 1998 bathymetric dataset was not fully available. Finally, the mean annual riverbed evolution of every 1-km-long segment in the main branch of the upper Tien River was estimated.

3.3 | Sand mining data

A local authority provided us with the annually licensed sand mining volume of the An Giang province in the upper Tien and Hau Rivers (from Tan Chau/Chau Doc to My Thuan/Can Tho) from 2008 to 2017

in 2017. The amount of sand mined annually was 1.3–3.1 Mm^3/year with a mean value of 1.7 Mm^3/year. We also collected sand mining volumes in the entire VMD of 7.75, 28 and 29.3 Mm^3/year in 2012, 2015 and 2018 from Bravard et al. (2013), Eslami et al. (2019), and Jordan et al. (2019), respectively. Among these three values, the amount of sand mined in the upper Tien and Hau Rivers was approximately 3.9, 13.3 (these two values were in the Tien River only, in both An Giang and Dong Thap provinces) and 13.43 Mm^3 (in both the Tien and Hau Rivers, including 3.36 Mm^3 from dredging in the Dong Thap province) in 2012, 2015 and 2018, respectively.

3.4 | Analytical methods

We firstly identified the trend and change point (year) and estimated the change rates of the discharge, water level and sediment load time series data using the non-parametric slope methods of Mann-Kendall, Pettitt and Sen (α = 0.05) (Kendall, 1938; Mann, 1945; Pettitt, 1979; Sen, 1968). We then partitioned the time series data into pre- and post-change periods based on the change years and applied the indicators of hydrologic alteration (IHA) and range of variability approach (RVA) to quantify the differences between the two periods. The IHA and RVA methods include 32 hydrologic indicators, which are categorized into magnitude, timing, duration and frequency (Richter et al., 1998).

We further employed the flow duration curve method (Vogel et al., 2007) to quantify the changes in the monthly and seasonal flow indicators between the pre- and post-change periods. The combination of the flow duration curve with the IHA method and RVA can provide comprehensive understanding of the monthly and seasonal flow regime alterations. We also used the flood frequency analysis method (England et al., 2018) to classify the floods into small, medium and large floods and then to quantify the changes in magnitude and frequency of these flood types.

3.5 | Two-dimensional hydrodynamics, sediment transport and bed evolution model

In examining the effects of sediment load reduction on riverbed incision and consequently on water level reduction, a coupled Telemac-2D (hydrodynamic model) and Sisyphe model (sediment transport and bed evolution model) in the Telemac Mascaret system, developed by the National Hydraulics and Environment Laboratory of Electricité de France, was established in the main rivers of the upper VMD, including islands and 1–2-km-wide floodplains (Figure 3(a)). A triangular mesh generated using the finite element method was employed in the simulated domain. The mesh had a grid spacing of 80 m in the wide segments and floodplains and 30–40 m in the narrow segments. We imposed the hourly subtidal discharges and daily SSCs of cohesive sediment at two upstream boundaries (i.e., Tan Chau and Chau Doc) and the hourly subtidal water levels and free sediment flow at two downstream boundaries (i.e., My Thuan and Can Tho). By imposing the hourly discharge and water level data, the influence of the tide on hydro-sediment-morpho dynamics of the study domain was well captured. The model simulated only the suspended load and bed evolution, whereas the bedload transport was not considered because the bed load was equal to only 1%–3% of the total annual load (Hackney et al., 2020; Jordan et al., 2019). The initial percentages of the bed materials were 95% fine sand (d_{50} = 214 μm) and 5% mud (d_{50} = 12.63 μm) (Gugliotta et al., 2017).

The coupled model was validated by tuning various physical and numerical parameters, using the water levels at Vam Nao, Cao Lanh and Long Xuyen (because discharge data were not available); SSCs at Vam Nao; and bed elevations at six cross-sections (i.e., CS-1–CS-6) (Figure 3(a)). We firstly validated the single hydrodynamic Telemac-2D model by mainly tuning the time step, friction coefficient and velocity diffusivity. Then, we re-validated the coupled model by further tuning critical shear stress for erosion, critical shear velocity for
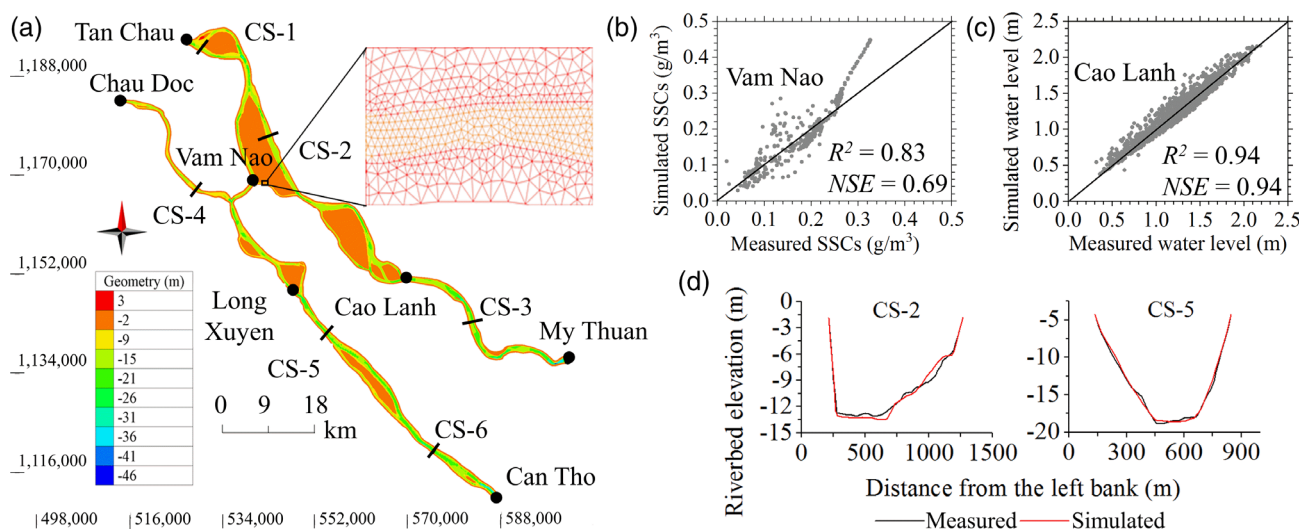
FIGURE 3 (a) Simulated domain, mesh, geometry and boundaries of the coupled Telemac-2D and Sisyphe model. (b)–(d) validation results: Relations between simulated and measured daily SSCs, daily water levels and riverbed elevations. These results indicate that the model was well validated. NSE = Nash-Sutcliffe coefficient

deposition, settling velocity and Krone-Partheniades constant (together with slight modification of the time step, friction coefficient and velocity diffusivity). The validation processes were performed for the period of 2014–2017. The goodness of the model was evaluated using the coefficient of determination (R^2) and Nash-Sutcliffe number, which are described in the Appendix S1. Figure 3(b–d) compare the simulated and measured data at typical positions, indicating that the model was well validated (e.g., $R^2 \geq 0.89$, Nash-Sutcliffe ≥ 0.81 for water levels and $R^2 = 0.83$, Nash-Sutcliffe $= 0.69$ for sediment concentrations).

Three scenarios were established based on the flow, sediment and riverbed elevation data from 2017 (the baseline) to predict the effects of the reduced sediment load on the water level responses through riverbed evolution. The simulation was performed for a 10 year period from 2017 to 2026 considering the tradeoff between the morphological responses after dam construction (33 years after Manwan and 15 years after Nuozhadu) and simulation time. In Scenario 1 (Sc1), the flow and sediment conditions were unchanged from 2017 to 2026. This scenario served as a reference to evaluate the effects of sediment reduction on the water level responses in Scenario 2 (Sc2) and Scenario

TABLE 3 Results of IHA analysis performed to determine flow regime alterations between the predam period (1980–1992) and postdam period (1993–2018) for Tan Chau

Indicator of hydrologic alteration	Mean discharge (m³/s)			Coefficient of variation		
	Predam	Postdam	Deviation magnitude/%	Predam	Postdam	Deviation magnitude/%
January	6586	6293	−293/−4	0.13	0.16	0.03/23
February	4169	4050	−119/−3	0.18	0.18	0/0
March	2525	2723	198/8	0.2	0.2	0/0
April	2112	2532	420/20	0.25	0.22	−0.03/−12
May	2800	3441	641/23	0.21	0.27	0.06/29
June	6821	6958	137/2	0.34	0.35	0.01/3
July	12 370	12 450	80/1	0.22	0.27	0.05/23
August	17 250	18 190	940/5	0.13	0.16	0.03/23
September	19 610	19 820	210/1	0.1	0.11	0.01/10
October	18 420	18 840	420/2	0.08	0.11	0.03/38
November	15 530	14 450	−1080/−7	0.11	0.16	0.05/45
December	10 440	10 040	−400/−4	0.14	0.18	0.04/29
1 day minimum	124	1578	1454/1173	0.63	0.41	−0.22/−35
3 day minimum	386	1705	1319/342	0.5	0.37	−0.13/−26
7 day minimum	871	1878	1007/116	0.29	0.31	0.02/7
30 day minimum	1707	2280	573/34	0.15	0.22	0.07/47
90 day minimum	2333	2705	372/16	0.17	0.2	0.03/18
1 day maximum	21 000	21 870	870/4	0.09	0.11	0.02/22
3 day maximum	20 930	21 810	880/4	0.09	0.11	0.02/22
7 day maximum	20 790	21 630	840/4	0.09	0.11	0.02/22
30 day maximum	20 110	20 630	520/3	0.09	0.11	0.02/22
90 day maximum	18 790	19 210	420/2	0.08	0.11	0.03/38
Base flow index	0.17	0.26	0.09/53	0.25	0.27	0.02/8
Date of minimum	118	97	−21/−18	0.08	0.05	−0.03/−38
Date of maximum	257	261	4/2	0.04	0.06	0.02/50
Low pulse count	5	4	−1/−20	0.40	0.79	0.39/98
High pulse count	2	1	−1/−50	0.41	0.42	0.01/2
Low pulse duration	19	29	10/53	0.54	0.70	0.16/30
High pulse duration	60	78	18/30	0.56	0.51	−0.05/−9
Fall rate	−269.7	−224	45.7/17	−0.13	−0.55	−0.42/−323
Rise rate	344.5	261.6	−82.9/−24	0.13	0.33	0.2/154
Number of reversals	76.6	100.9	23.4/31	0.10	0.19	0.09/90

Note: deviation magnitude = postdam − predam; % = deviation magnitude/predam × 100%.

(Sc3). In Sc2 and Sc3, the flow regimes were unchanged from 2017 to 2026 and the sediment loads at the upstream boundaries were reduced by 17.5% and 84.8%, respectively, in 2026 compared to 2017. Sc2 was established based on the analysis of long-term monthly sediment reduction in the VMD by Binh et al. (2020). Sc3 was based on Kondolf et al. (2014), who estimated that only 4% of the predam sediment load of the Mekong will reach the VMD if all 133 dams are built. In other words, the sediment load of the VMD with 133 completed dams will be 6.7 Mt/year (=4% × 166.7 Mt/year, where 166.7 Mt/year is the predam sediment load of the VMD [Binh et al., 2020]), which is reduced by 84.8% of the 2017 sediment load (43.9 Mt/year).

4 | RESULTS

## 4.1 | Differences in spatiotemporal patterns of long-term discharge alterations

The IHA analysis results showed that the flow regime alterations in the VMD were different between the dry and flood seasons (Tables 3 and 4; Figure 4). The Mann-Kendall test and IHA analysis revealed that the dry season discharges, for example, in March–May, at Tan Chau and Chau Doc increased significantly ($\alpha < 0.05$), whereas the flood season discharges, for example, in

TABLE 4 Results of IHA analysis performed to determine flow regime alterations between the predam period (1980–1992) and postdam period (1993–2018) for Chau Doc

Indicator of hydrologic alteration	Mean discharge (m³/s)			Coefficient of variation		
	Predam	Postdam	Deviation magnitude/%	Predam	Postdam	Deviation magnitude/%
January	1352	1289	−63/−5	0.07	0.11	0.04/57
February	709	747	38/5	0.06	0.08	0.02/33
March	312	473	161/52	0.06	0.05	−0.01/−17
April	356	464	108/30	0.07	0.06	−0.01/−14
May	426	608	182/43	0.06	0.11	0.05/83
June	1259	1313	54/4	0.19	0.19	0/0
July	2689	2640	−49/−2	0.17	0.22	0.05/29
August	4183	4667	484/12	0.15	0.16	0.01/7
September	5560	5608	48/1	0.13	0.13	0/0
October	5426	5611	185/3	0.10	0.13	0.03/30
November	4512	3944	−568/−13	0.13	0.17	0.04/31
December	2520	2333	−187/−7	0.11	0.15	0.04/36
1 day minimum	−349	135	484/139	0.15	0.20	0.05/33
3 day minimum	−273	201	474/174	0.13	0.18	0.05/38
7 day minimum	−105	262	367/350	0.10	0.15	0.05/50
30 day minimum	193	386	193/100	0.04	0.06	0.02/50
90 day minimum	327	472	145/44	0.05	0.06	0.01/20
1 day maximum	6205	6341	136/2	0.13	0.12	−0.01/−8
3 day maximum	6182	6323	141/2	0.13	0.12	−0.01/−8
7 day maximum	6129	6275	146/2	0.13	0.13	0/0
30 day maximum	5869	6029	160/3	0.12	0.13	0.01/8
90 day maximum	5360	5432	72/1	0.10	0.12	0.02/20
Base flow index	0.42	0.51	0.09/21	0.11	0.16	0.05/45
Date of minimum	111	94	−17/−15	0.09	0.07	−0.02/−22
Date of maximum	269	270	1/0	0.05	0.05	0/0
Low pulse count	7	6	−1/−14	0.38	0.78	0.4/105
High pulse count	1	1	0/0	0.46	0.45	−0.01/−2
Low pulse duration	10	5	−5/−50	0.46	0.75	0.29/63
High pulse duration	78	82	4/5	0.36	0.42	0.06/17
Fall rate	−83.5	−77.8	5.7/7	−0.10	−0.69	−0.59/−590
Rise rate	93.7	80.4	−13.3/−14	0.10	0.47	0.37/370
Number of reversals	83.5	111.2	27.7/33	0.16	0.24	0.08/50

Note: deviation magnitude = postdam − predam; % = deviation magnitude/predam × 100%.
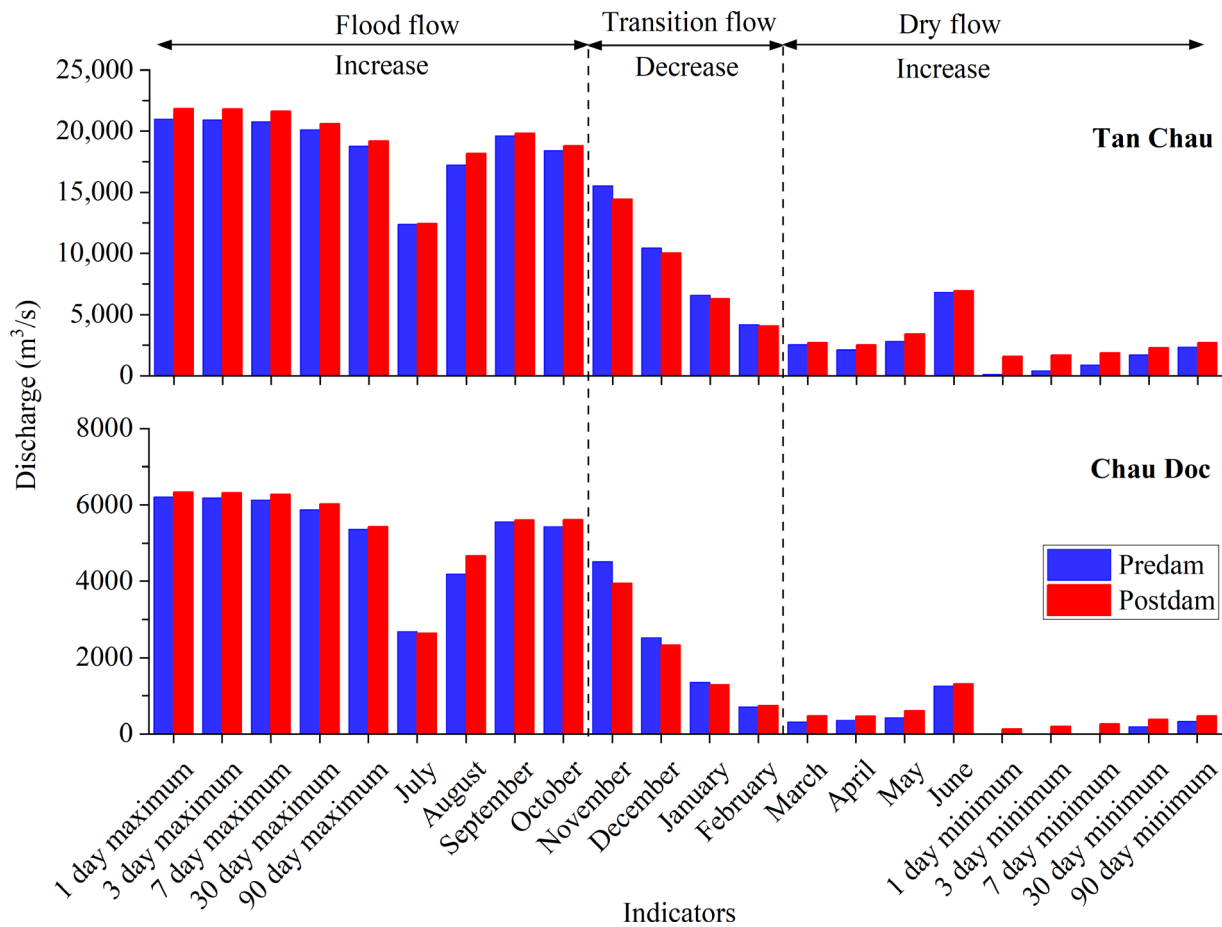
FIGURE 4 Changes in the extreme and monthly discharges between the predam and postdam periods at Tan Chau and Chau Doc from the IHA results. The postdam discharges increased in the flood and dry seasons but decreased in the transition period (end of the flood season and beginning of the dry season)

August–October, increased slightly (without statistical significance). The change years were around 1993, as identified using the Pettitt test. Therefore, the long-term discharge data were divided into the predam period (pre-1992) and postdam period (1993–2018) for further analyses. This division has been utilized by various researchers (e.g., Lauri et al., 2012; Lu & Siew, 2006).

4.1.1 | Alterations in extreme discharges

The annual daily maximum discharges (1-, 3- and 7-day maxima) at both Tan Chau and Chau Doc increased from the predam to postdam period (Figures 4 and 5; Tables 3 and 4). The flood peak was delayed in the postdam period. Flood frequency analysis at Tan Chau revealed increases in the postdam annual daily maximum discharges at all exceedance probabilities compared to the predam values (Figure 5). The annual daily maximum discharge increases were greater in the large floods (floods with ≤10% probability or greater than 10 year return periods) than in the small and medium floods (floods with >10% probability or less than 10 year return periods). However, the annual daily maximum discharge at Chau Doc in the

postdam period increased in the small and medium floods but decreased in the large floods. On the other hand, the annual daily minimum discharges at both Tan Chau and Chau Doc in the postdam period increased significantly ($\alpha < 0.01$ in the Mann-Kendall test) and even exceeded the high RVA boundary (Figure 5). Moreover, the annual daily minimum discharges at Tan Chau and Chau Doc occurred 21 and 17 days earlier, respectively, in the postdam period (Tables 3 and 4).

4.1.2 | Alterations in seasonal and monthly discharges

The IHA and flow duration curve results revealed slight increases in the flood season discharge (e.g., in August–October and 30- and 90-day maxima) at Tan Chau and Chau Doc in terms of both magnitude and duration from the predam to postdam period (Figures 4 and 6; Tables 3 and 4). The greatest increase was in August, with rates of 45.2 and 18.2 m^3/s/year at Tan Chau and Chau Doc, respectively, from 1980 to 2018. Additionally, the high pulse duration in the postdam period increased by 30% and 5% at Tan Chau and Chau Doc, respectively.
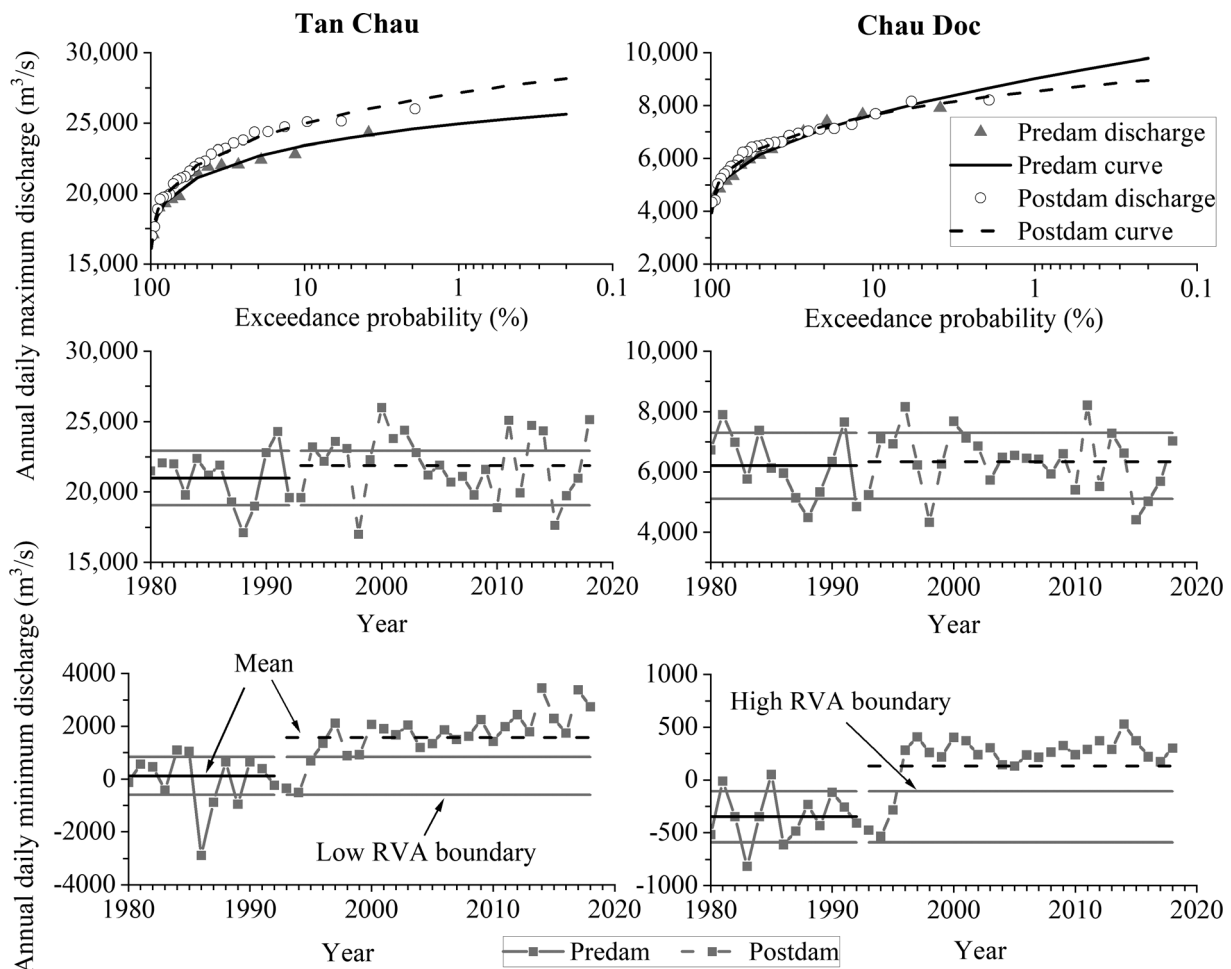
FIGURE 5 Identification of long-term alterations of the 1–day maximum and minimum discharges at Tan Chau and Chau Doc according to IHA, RVA and flood frequency analysis

On the other hand, the dry season discharge improved substantially at these two stations, with increased magnitude and decreased frequency and duration (Figures 4 and 6; Tables 3 and 4). The greatest increases in the dry season discharge occurred in the 30- and 90-day minima and in April–May. The dry season discharges at Tan Chau and Chau Doc increased by 2%–34% and 4%–100%, respectively. Notably, the discharges at the end of the flood season (November–December) and the beginning of the dry season (January–February) decreased at Tan Chau and Chau Doc in the post-dam period (Figures 4 and 6; Tables 3 and 4). The decrease rates from 1980 to 2018 during these months ranged from −4.3 to −41.4 m^3/s/year at Tan Chau and from −5.3 to −30 m^3/s/year at Chau Doc.

4.2 | Differences in spatiotemporal patterns of long-term water level alterations

There were spatiotemporal differences in the alterations of the long-term water levels in the VMD. The annual daily maximum and mean monthly water levels in the flood season in the upper delta (at Tan Chau and Chau Doc) decreased substantially (Figure 7). The reduction

was statistically significant in September at Tan Chau ($\alpha < 0.05$) and Chau Doc ($\alpha < 0.1$). Significant decreases ($\alpha < 0.01$) were also found at My Thuan in the lower delta in July–December (Table S1). For instance, the mean water level in September at My Thuan decreased by −12% from the predam to postdam period (Table 5) and it decreased at a rate of −9 mm/year from 1980 to 2018 ($\alpha < 0.01$). However, the annual daily maximum and mean monthly water levels in the flood season at Can Tho increased significantly ($\alpha < 0.01$, see Table S2; Figure 7). The increase rate was up to 7 mm/year (in August) from 1980 to 2018 ($\alpha < 0.01$).

In the dry season, the mean monthly water level increased in March–May at Tan Chau (not statistically significant), in February–May at Chau Doc ($\alpha < 0.05$ in March and April) and in January–June at Can Tho ($\alpha < 0.01$) from 1980 to 2018. However, the mean water level decreased statistically in June at Tan Chau ($\alpha < 0.05$) and in January and June at My Thuan ($\alpha < 0.05$). It decreased by −12% and −46% at Tan Chau and My Thuan, respectively, from the predam to postdam period (Figure 7; Table 5). The annual daily minimum water level at My Thuan decreased at a rate of −2 mm/year in 1980–2018 and by −44% in the postdam period. Moreover, the annual daily mean water levels at Tan Chau, Chau Doc and My Thuan decreased by
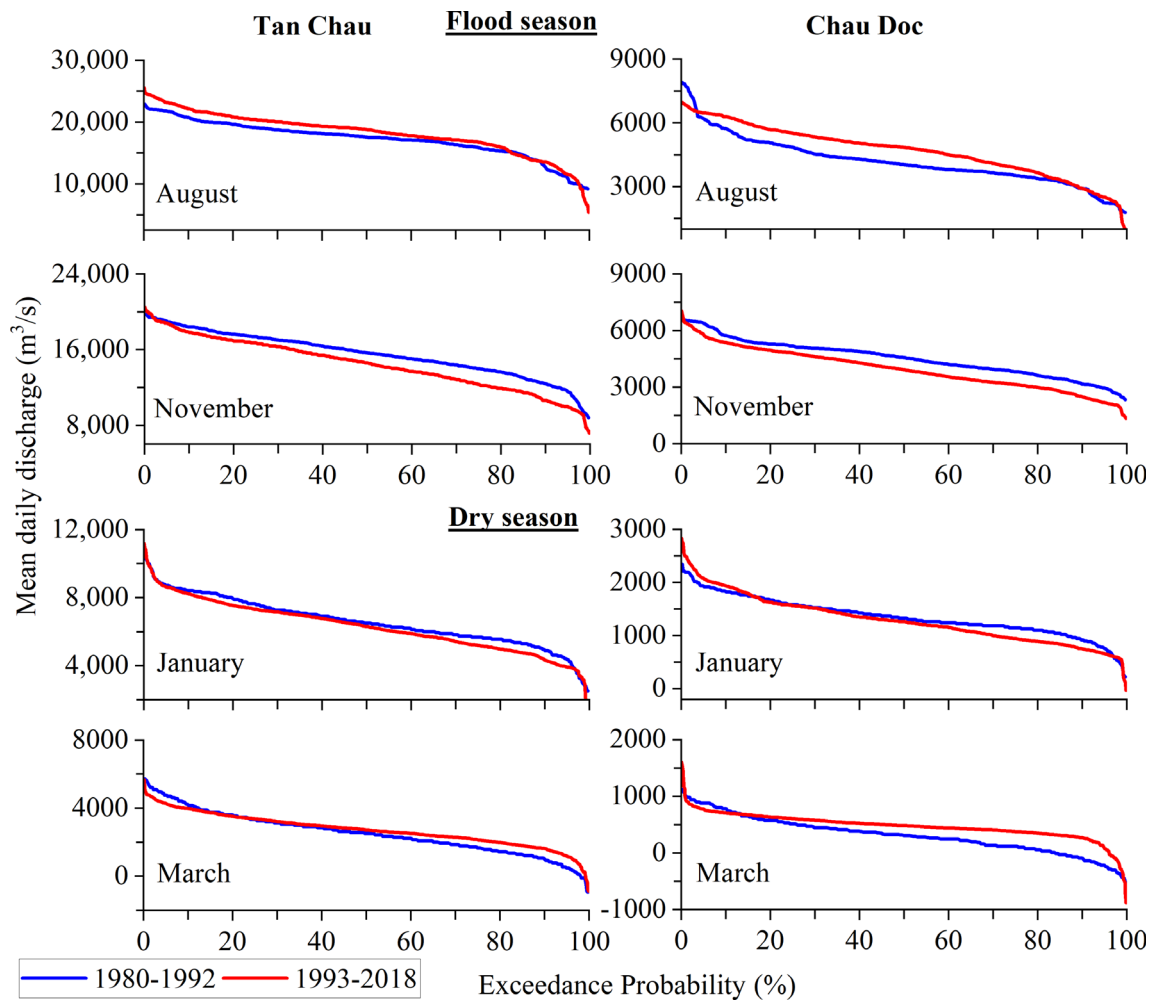
FIGURE 6 Monthly flow duration curves at Tan Chau and Chau Doc in the flood and dry seasons between the predam and postdam periods

−9.2, −5.4 and −4.1 mm/year, respectively, from 1980 to 2015, starting from 2002 at Tan Chau ($\alpha = 0.05$) and Chau Doc ($\alpha > 0.1$) and from 2003 at My Thuan ($\alpha < 0.01$, Table S1). Additionally, the mean monthly water level decreased at the end of the flood season (November–December) and the beginning of the dry season (January–February) at Tan Chau, Chau Doc and My Thuan ($\alpha < 0.05$) (Figure 7). The greatest reduction was at My Thuan, for example, by −3 mm/year in January ($\alpha < 0.05$) in 1980–2018 (Table S1).

4.3 | Accelerated riverbed incision, decreased sediment load and increased sand mining

The riverbeds in the upper Tien River and Vam Nao channel incised significantly from 1998 to 2017 (Figure 8). The mean incision rates of the river thalweg were −0.33 and −1.24 m/year in 1998–2014 and 2014–2017 respectively. Riverbed incision was observable in the entire river, rather than being limited to the thalweg and cross-sections (Figure 8(a–d)). The maximum annual incision depth was −0.54 m/year in 1998–2014 and reached −0.97 m/year in 2014–2017 (Figure 8(e)). We estimated the net annual incision

volume of the entire region to be −16.7 and −52.5 Mm^3/year in 1998–2014 and 2014–2017, equivalent to mean annual incision depths of −0.16 and −0.5 m/year, respectively. The incision was higher from Tan Chau to Cu Lao Tay island, in the Vam Nao channel and around 20 km upstream from My Thuan than in the remaining areas (Figure 8). For instance, the annual riverbed incision of the last 20 km (upstream from My Thuan) was estimated to be −3.4 and −6.4 Mm^3/year, equivalent to a mean annual incision depth of −0.19 and − 0.38 m/year in 1998–2014 and 2014–2017, respectively.

The sediment load in the VMD is the summation of the respective sediment loads at Tan Chau and Chau Doc. The Mann-Kendall test showed that the monthly and annual sediment loads in the delta decreased significantly ($\alpha < 0.001$) (Figure S3), from 166.7 Mt/year in the predam period to 57.6 Mt/year in the postdam period (−65.4%). The sediment loads were especially low after 2009, such as 29.6 Mt/year in 2010 and 27.6 Mt/year in 2015. Similarly, the sediment loads at other stations along the Mekong decreased sharply (Figure S3), especially at Luang Prabang ($\alpha < 0.001$) and Nong Khai ($\alpha < 0.001$). Notably, no significant trends were found at Mukdahan or Khong Chiam due to the over-estimation of the sediment loads from 2009 to 2013 because of the limitations of the sampling device (Koehnken, 2014).
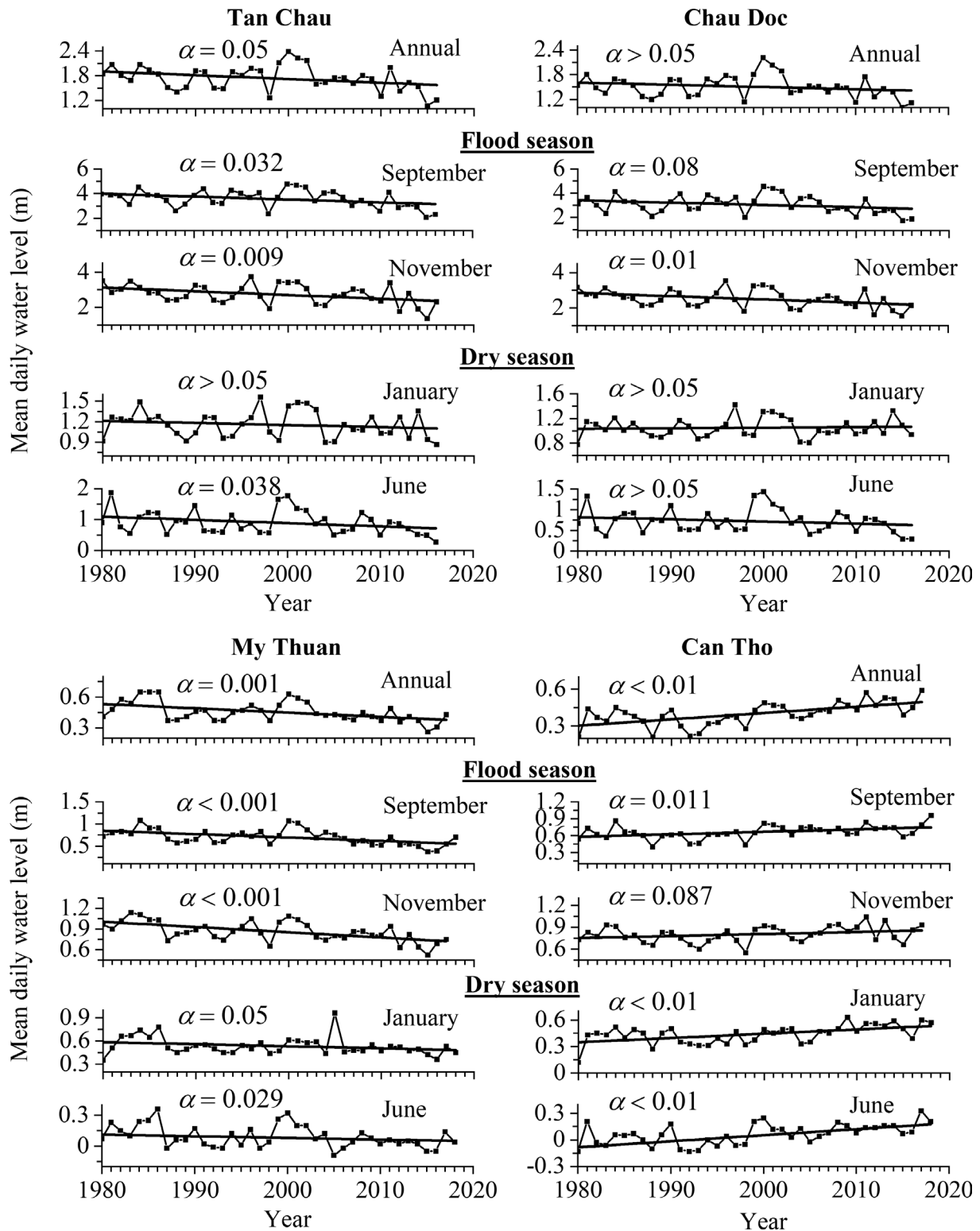
FIGURE 7 Differences in spatiotemporal patterns of long-term mean daily water level alterations in the flood and dry seasons in the VMD

Although the sediment supply from the Mekong decreased, sand mining within the VMD increased (Figure S4). In the upper Tien and Hau Rivers, sand mining volume in the An Giang province decreased after 2009 but gradually increased after 2011 (Figure S4a). In particular, the amount of sand mined increased from 1.3 Mm^3 in 2011 to 1.9 Mm^3 in 2017. Similarly, the sand mining volumes in the An Giang and Dong Thap provinces collected from Bravard et al. (2013), Eslami et al. (2019), and Jordan et al. (2019) substantially increased from approximately 3.9 Mm^3 in 2012 to 13.3 Mm^3 in 2015 and 13.43 Mm^3 in 2018 (Figure S4b).

TABLE 5 Changes in the water level (in metres) between the predam and postdam periods in the VMD

Indicator of hydrologic alteration	Tan Chau			Chau Doc		
	Predam	Postdam	Deviation magnitude/%	Predam	Postdam	Deviation magnitude/%
January	1.18	1.15	−0.03/−3	1.04	1.06	0.02/2
February	0.8	0.81	0.01/1	0.72	0.78	0.06/8
March	0.57	0.61	0.04/7	0.51	0.6	0.09/18
April	0.42	0.48	0.06/14	0.38	0.46	0.08/21
May	0.46	0.49	0.03/7	0.38	0.46	0.08/21
June	0.98	0.87	−0.12/−12	0.74	0.72	−0.02/−3
July	1.81	1.77	−0.04/−2	1.35	1.36	0.01/1
August	2.87	2.88	0.01/0.5	2.14	2.36	0.22/10
September	3.68	3.51	−0.17/−5	3.09	3.05	−0.04/−1
October	3.69	3.64	−0.05/−1	3.3	3.3	0/0
November	2.91	2.65	−0.26/−9	2.66	2.44	−0.22/−8.2
December	1.84	1.74	−0.1/5	1.64	1.59	−0.05/−3
1 day minimum	0.12	0.16	0.04/33	0.05	0.11	0.06/120
1 day maximum	4.03	4	−0.03/−1	3.57	3.59	0.02/1
Indicator of hydrologic alteration	My Thuan			Can Tho		
	Predam	Postdam	Deviation magnitude/%	Predam	Postdam	Deviation magnitude/%
January	0.57	0.52	−0.05/−9	0.4	0.45	0.05/13
February	0.41	0.37	−0.04/−10	0.25	0.34	0.09/36
March	0.28	0.26	−0.02/−7	0.14	0.24	0.1/71
April	0.17	0.15	−0.02/−12	0.04	0.14	0.1/250
May	0.11	0.06	−0.05/−46	−0.02	0.07	0.09/450
June	0.13	0.07	−0.06/−46	0.01	0.09	0.08/800
July	0.32	0.25	−0.07/−22	0.19	0.28	0.09//47
August	0.52	0.47	−0.05/−10	0.37	0.5	0.13/35
September	0.76	0.67	−0.09/−12	0.61	0.68	0.07/11
October	0.96	0.91	−0.05/−5	0.8	0.89	0.09/11
November	0.94	0.82	−0.12/−13	0.78	0.81	0.03/4
December	0.74	0.66	−0.08/−11	0.57	0.63	0.06/11
1 day minimum	−0.23	−0.33	−0.1/−44	−0.35	−0.29	0.06/17
1 day maximum	1.2	1.19	−0.01/−1	1.03	1.21	0.18/18

Note: deviation magnitude = postdam − predam; % = deviation magnitude/predam × 100%.

4.4 | Modelling the effect of riverbed incision on the reduced water level

The influence of riverbed incision caused by sediment reduction on the reduced water level in the upper Tien River was clearly found in the coupled 2D model results (Figure 9). We estimated that the net riverbed incision by the end of 2026 was −1.27 m in Sc1 and it became −1.48 m in Sc2 and −2.04 m in Sc3. Compared to Sc1, the riverbed was incised by an additional 17% and 61% under 17.5% and 84.8% sediment load reductions, respectively. Consequently, the water level decreased significantly in 2017–2026 (Figure 9(c)). The mean monthly water level in April 2026 (April had the lowest water level in a year) was decreased by −0.08 to −0.47 m, −0.12 to

−0.54 m and − 0.21 to −0.68 m compared to that in April 2017 in Sc1, Sc2 and Sc3, respectively. Compared to Sc1, it decreased by −15% to −50% and −44% to −163% under 17.5% and 84.8% sediment load reductions, respectively.

5 | DISCUSSION

5.1 | Drivers of discharge and morphological changes

The annual daily maximum and flood season discharges and flood durations at Tan Chau and Chau Doc were slightly greater in the
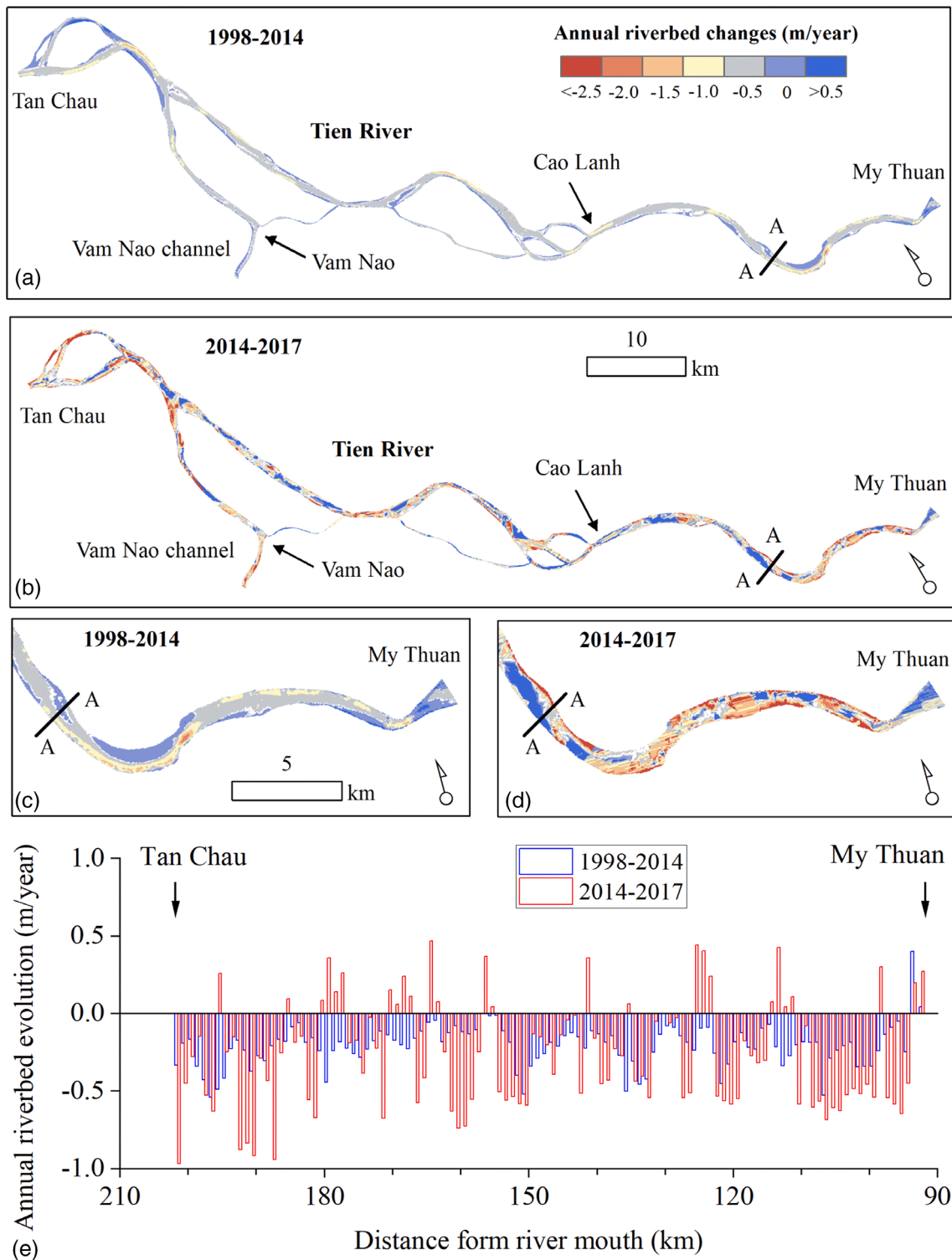
FIGURE 8 Comparison of the annual morphological changes between 1998–2014 and 2014–2017 in the upper Tien River and the Vam Nao channel. (a)–(d) 3D maps. (e) Mean riverbed level changes for every 1-km-long segment of the main branch from Tan Chau to My Thuan

postdam period than in the predam period (Figures 4–6; Tables 3 and 4). These increases are in line with the increases in the annual daily maximum discharge at Chiang Saen, Mukdahan and Kratie by 6.1%, 18.7% and 4.4%, respectively, and are consistent with the results of other studies of the Mekong and other river basins (e.g., Delgado

et al., 2010; Lu & Siew, 2006; Yang et al., 2004). The discharge increases along the Mekong occurred mainly in 1993–2008 when the mean rainfall increased by 5% in the Mekong basin (Figure S5). Therefore, climate conditions, that is, the Western North-Pacific, East Asian and Indian monsoons, which generate intense rainfall in the Mekong
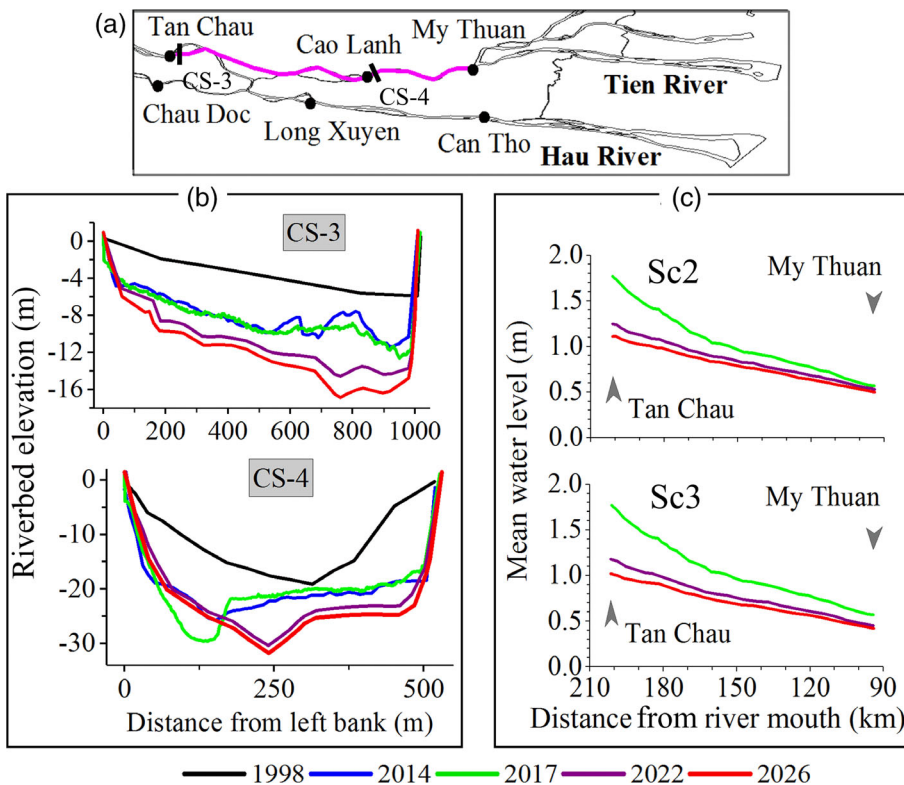
FIGURE 9 (a) General map of the VMD showing hydrological stations. (b) Cross-sections showing riverbed evolution from 1998 to 2026 in Sc3. The riverbed elevation was measured in 1998, 2014 and 2017 and simulated in 2022 and 2026. (c) Simulated water level reductions caused by riverbed incision along the upper Tien River

basin (Darby et al., 2013), were likely drivers of the discharge increases. Moreover, climate change, which has been predicted to increase the magnitudes and frequencies of extreme events (Hoang et al., 2016; Hoanh et al., 2010), may be another controlling factor. This finding indicates that dams completed before 2008, which have small reservoir capacities relative to the total discharge of the Mekong, may have limited capacities to regulate the runoff from the Mekong basin, especially in extreme events.

In the dry season, the annual daily minimum and monthly discharges were significantly increased at Tan Chau and Chau Doc in the postdam period (Figures 4–6; Tables 3 and 4). Our results are consistent with the significant increases in the dry season discharges previously observed at Chiang Saen and Stung Treng, which were attributed to dam operations (D. Li et al., 2017; Räsänen et al., 2017). Moreover, irrigation withdrawals along the lower Mekong may reduce the dry season discharge, but the effect is slight (Haddeland et al., 2006) because of the increased postdam discharge in the dry season.

The riverbed in the upper Tien River and Vam Nao channel has severely incised (Figure 8). The annual incision volume and depth in 2014–2017 (−52.5 Mm³/year and −0.5 m/year, respectively) were more than three times greater than those in 1998–2014 (−16.7 Mm³/year and −0.16 m/year, respectively). Riverbed incision is not limited to the VMD, but rather also occurs in alluvial reaches in Thailand and Cambodia (Hackney et al., 2020; Rubin et al., 2015). Moreover, riverbank erosion from the Jinghong dam to Chiang Saen and from Vientiane to Nong Khai has been documented by Bravard et al. (2014) and Kummu et al. (2008). We found a link between the riverbed incision in the upper VMD and the reduced sediment load and accelerated sand

mining in the Mekong (Figures 8, Figures S3 and S4). Our findings are consistent with the results reported by Binh et al. (2020), Eslami et al. (2019), Hackney et al. (2020), and Jordan et al. (2019). The sediment load of the Mekong has significantly decreased since 1993, when the Manwan dam was completed, and was substantially low after 2009, when the two largest dams in the Lancang cascade (i.e., Xiaowan and Nuozhadu, see Table 1) began operation (Figure S3). Climate change, which has shifted the tracks of tropical cyclones, has also been reported to reduce the sediment load of the Mekong (Darby et al., 2016). We anticipate from the coupled numerical model that the riverbed incision in the upper VMD may increase by 17% and 61% by 2026 under reduction of the sediment supply from the Mekong by 17.5% and 84.8%, respectively, compared to the unchanged sediment load in 2017–2026. As the second driver, sand mining in the upper VMD increased from 3.9 Mm³ in 2012 to 13.43 Mm³ 2018 (Figure S4b), accounting for 23.4% and 25.6% of riverbed incision in 1998–2014 and 2014–2017, respectively. It is worth noting that the actual volume of sand mining might be much larger than the reported values because of illegal mining activities by both licensed miners and local people (Binh et al., 2020; Bravard et al., 2013).

5.2 | Effects of riverbed incision on water level reduction in the VMD

The annual daily maximum and flood season water levels at Tan Chau, Chau Doc and My Thuan decreased (Figure 7; Table 5), although the

corresponding discharges increased (Figures 4–6; Tables 3 and 4). Notably, the water level reduction was statistically significant in September, November and December at Tan Chau and Chau Doc and in July–December at My Thuan (Table S1). Similarly, the annual mean water level and that in June at Tan Chau ($\alpha < 0.05$) and the annual mean ($\alpha < 0.01$) and monthly water level in January and June ($\alpha < 0.05$) at My Thuan decreased statistically, whereas the respective discharges of the Tien River increased significantly. These decreases in the water level cannot be explained by sea level rise (Eslami et al., 2019) and dam operations that are attributable to the increased

dry season water level through the increased discharges. Moreover, irrigation expansion is likely not the cause because it did not reduce the dry season discharge of the Mekong. Therefore, we argue that these decreases in the water level are mainly driven by riverbed incision caused by the decreased sediment load and accelerated sand mining. Riverbed incision is significant upstream from My Thuan in the Tien River from 1998 to 2017 (Figure 8) and upstream from Can Tho in the Hau River (Eslami et al., 2019). Water level reduction is more significant at My Thuan because of significant riverbed incision around this area, as estimated by Jordan et al. (2019). Although data
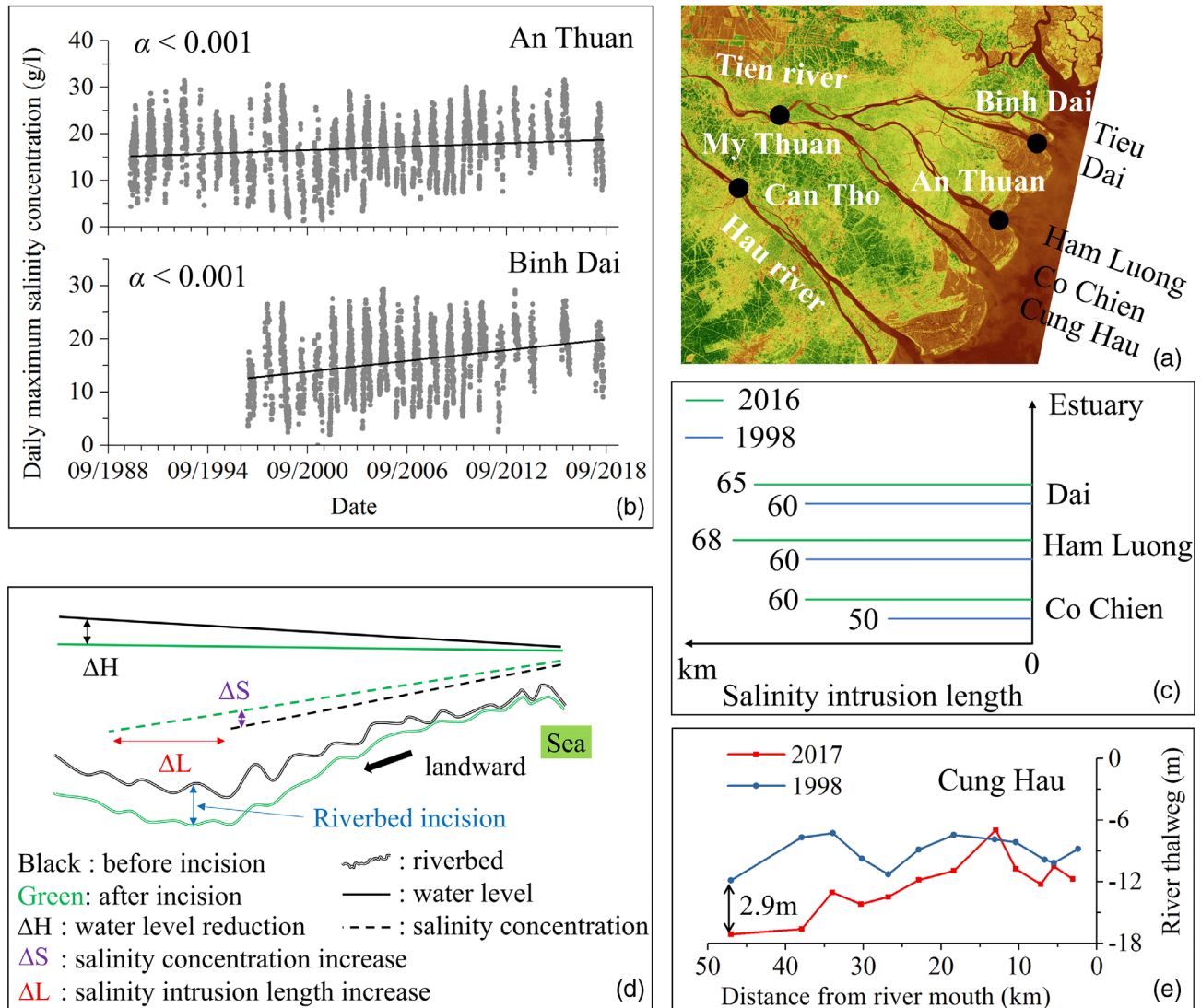
FIGURE 10 (a) Map of the VMD location. (b) Increases in long-term daily maximum salinity concentrations in the estuaries of the Tien river from the 1990s to 2018. (c) Increases in salinity intrusion length of 4 g/L between 1998 and 2016. Salinity intrusion lengths were simulated using a semi-two-dimensional Mike 11 model (i.e., one dimensional in the river channels and quasi-two dimensions in the floodplains by representing rice field compartments as linked channels connecting with the main channels), adopted from Mai et al. (2018). The model contains five upstream boundaries using hourly discharge and zero salinity and 59 downstream boundaries (at river mouths) using hourly water level and odd hourly salinity concentration. The model was validated using the hydrologic, salinity, topographic and bathymetric data measured in 2016. (d) Conceptual model of increasing salinity intrusion (both magnitude and length) caused by riverbed incision–induced water level reduction. Riverbed incision reduces the water surface gradient, leading to increasing salinity. (e) Incision of the river Thalweg in the Cung Hau branch of the Tien River between 1998 and 2017. The figure schematises that riverbed incision-induced water level reduction is likely one of the main causes of the increased salinity intrusion in the Tien river besides tidal amplification and riverbed incision-induced tidal velocity increase (Eslami et al., 2019)

are not available before 2008, sand mining in the upper VMD is accelerating (Figure S4), which is in agreement with the decreases in the annual mean water levels at Tan Chau, Chau Doc and My Thuan, starting from 2002 to 2003 (Table S1). Numerically, Binh et al. (2018) revealed that the rates of riverbed incision in the upper Tien and Hau Rivers exceeded the rates at which the water depth increased due to the increased discharge. Using a coupled numerical model, we anticipate that the mean water level in April of the upper Tien and Hau Rivers might be reduced by −15% to −50% and −44% to −163% under 17.5% and 84.8% sediment load reductions by 2026, respectively (Figure 9). Therefore, we speculate that the dry season water levels in January and February at Tan Chau and in January, February and May at My Thuan might be statistically reduced in the next decades, although the current reductions were not statistically significant. Consequently, the floodplains may be disconnected from the rivers (Park et al., 2020).

The dry season water levels at Can Tho increased statistically because of the respective discharge increases in the Hau River under

insignificant riverbed changes downstream from Can Tho (Eslami et al., 2019). Statistical increases in the flood season water levels at Can Tho have been well documented by the shift of the flood wave from upstream due to high-dyke system (Triet et al., 2017).

5.3 | Implications for salinity intrusion

Figure 10(b) shows significant increases ($\alpha < 0.001$) in the daily maximum salinity concentrations at An Thuan (in 1990–2018) and Binh Dai (in 1997–2018) in the estuaries of the Tien River, by rates of 0.4 and 0.8 g/L/year, respectively. The salinity increased not only the magnitude, but also the length of intrusion (Figure 10(c)). For instance, the 4 g/L contour line in the Co Chien–Cung Hau branches of the Tien River increased from 50 km in 1998 to 60 km in 2016. We observed a linkage between the increased salinity intrusion and accelerated riverbed incision (Figures 8, 9 and 10(e)), which caused water level
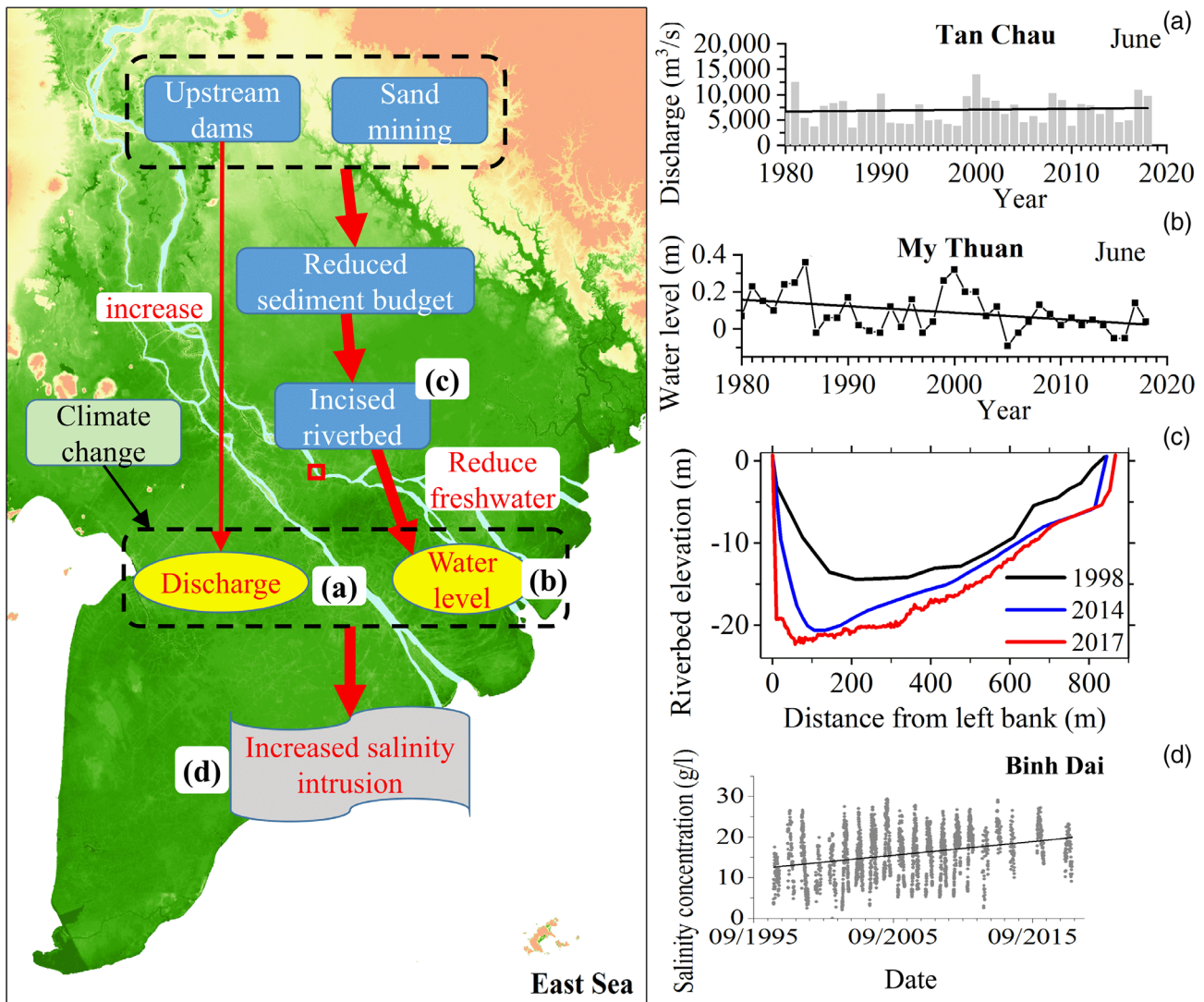
FIGURE 11 Summary of the effects of riverbed incision on the water level reduction and increase in salinity intrusion. The locations of the hydrological and salinity stations are shown in Figures 1 and 10(a). (a) Increase in discharge and (b) decrease in water level in the VMD because of (c) riverbed incision caused by upstream dams and sand mining. (d) Subsequent increase in salinity intrusion

reduction (Figure 7) especially at My Thuan in the dry season (Table 5). Figure 11 summarizes our findings. Our observations are in agreement with the finding of Eslami et al. (2019), who found that riverbed incision strongly affects the salinity intrusion in the VMD. Figure 10(d) shows a schematic diagram of the increased salinity intrusion caused by riverbed incision-induced water level reduction. When the water level decreases in the landward areas, the water surface gradient between sea and land decreases, which increases the salinity intrusion.

6 | UNCERTAINTIES

The present study may include some uncertainties. First, morphological changes may have led to misestimates of the hourly discharge at the hydrological stations in the VMD based on the hourly water level and consequently may have influenced the presented trends. However, the relationship between hourly discharge and water level was frequently updated using an acoustic Doppler current profiler, for instance, four times a year in January, April, July and October at My Thuan and Can Tho (Ha et al., 2018). Second, the use of all available daily data to develop stage-discharge rating curves in this study may have yielded under- or over-estimates of the discharge in the predam period. Furthermore, the division into the rising and falling stages when developing the rating curves may have involved some limitations because the tidal influence on the flow is stronger in January–March than in October–December. Nevertheless, the predam daily discharge data were also used to develop the rating curves. Moreover, the coefficients of determination of the developed rating curves were high ($R^2 > 0.95$). Therefore, the estimated discharge data were of sufficient quality to use in the analyses. Third, there may have been some limitations in the long-term sediment load data originating from the sampling device itself or the inconsistency of the sampling methods at the analysed stations in different periods, which may have affected the trends presented in this paper. In particular, the sediment loads at the stations upstream from the VMD were obtained from two sources: the hydrological (HYMOS) dataset and Water Quality Monitoring Network (WQMN) dataset (Wang et al., 2011). The HYMOS dataset was obtained using a depth-integrated method, whereas the WQMN dataset was acquired using a point measurement method (i.e., at 0.3 m below the water surface) with a low sampling frequency (i.e., at monthly intervals). However, the WQMN dataset was converted into the HYMOS dataset using linear regression (Wang et al., 2011) before conducting the analysis. Fourth, the 2D coupled model was able to capture large-scale patterns but not local riverbed incision because we did not include the effects of sand mining in the simulation.

7 | CONCLUSIONS

We examined the spatiotemporal alterations of the flow regimes in the VMD by analysing the long-term daily, monthly, annual and extreme discharge and water level along the Tien and Hau Rivers over a 39 year period from 1980 to 2018 and further analysed the long-term annual sediment load, river bathymetric data and daily salinity concentrations. Insights into the effect of riverbed incision on water level reduction was simulated by a couple Telemac-2D and Sisyphe model. The main conclusions are as follows.

1. The annual daily maximum and flood season discharges in the delta increased by 1%–5% at Tan Chau and 1%–12% at Chau Doc from the predam period to the postdam period, but the corresponding water levels decreased by up to −9% at Tan Chau, −8.2% at Chau Doc and −22% at My Thuan.

2. In the dry season, the mean discharge in June increased by 2% in the Tien River at Tan Chau and 4% in the Hau River at Chau Doc in the postdam period. However, the mean water level in June decreased by −12% at Tan Chau, −3% at Chau Doc and −46% at My Thuan. Notably, the annual mean water level and that in June at Tan Chau and the annual mean and monthly water levels in January and June at My Thuan in the Tien River decreased statistically, whereas the corresponding discharges increased substantially.

3. The riverbeds in the upper Tien and Hau Rivers experienced significant incision. The mean annual incision rate has increased by more than three times, from −0.16 m/year (−16.7 Mm^3/year) in 1998–2014 to −0.5 m/year (−52.5 Mm^3/year) in 2014–2017. This accelerated riverbed incision is likely due to the reduced sediment load of the VMD (from 166.7 Mt/year in the predam period to 57.6 Mt/year in the postdam period) and the increased sand mining (from 3.9 Mm^3 in 2012 to 13.43 Mm^3 in 2018). We numerically estimated that the riverbed incision in 2026 may be increased by 17% and 61% under 17.5% and 84.8% sediment supply reduction, respectively.

4. We observed that riverbed incision was the main cause of the statistically decreased water level in June at Tan Chau and in January and June–October at My Thuan in the Tien River, although the discharge increased. The decreased water level in the dry season in the Tien River was likely one of the main causes of the enhanced salinity intrusion. Therefore, the sustainable development of the VMD requires appropriate management of riverbed incision such as effective sand mining regulation and integrated management of the Mekong river basin.

CONFLICT OF INTEREST

The authors declare no conflicts of interest.

DATA AVAILABILITY STATEMENT

The data that support the findings of this study are available upon reasonable request from the corresponding author. The data are not publicly available due to privacy or ethical restrictions.

ORCID

Doan Van Binh https://orcid.org/0000-0002-7687-0550

Sameh A. Kantoush https://orcid.org/0000-0003-0919-5097

Tetsuya Sumi https://orcid.org/0000-0002-1423-7477

Trieu Anh Ngoc https://orcid.org/0000-0003-0324-5516

Tran Dang An https://orcid.org/0000-0002-6835-0416

REFERENCES

Anthony, E. J., Brunier, G., Besset, M., Goichot, M., Dussouillez, P., & Nguyen, V. L. (2015). Linking rapid erosion of the Mekong River Delta to human activities. *Scientific Reports*, 5, 14745.

Arias, M. E., Cochrane, T. A., Kummu, M., Lauri, H., Holtgrieve, G. W., Koponen, J., & Piman, T. (2014). Impacts of hydropower and climate change on drivers of ecological productivity of Southeast Asia's most important wetland. *Ecological Modelling*, 272, 252–263.

Batalla, R. J., Gomez, C. M., & Kondolf, G. M. (2004). Reservoir-induced hydrological changes in the Ebro River basin (NE Spain). *Journal of Hydrology*, 290, 117–136.

Besset, M., Anthony, E. J., & Bouchette, F. (2019). Multi-decadal variations in delta shorelines and their relationship to river sediment supply: An assessment and review. *Earth-Science Reviews*, 193, 199–219.

Best, J. (2019). Anthropogenic stresses on the world's big rivers. *Nature Geoscience*, 12, 7–21.

Binh, D. V., Kantoush, S., Mai, N. P., & Sumi, T. (2018). Water level changes under increased regulated flows and degraded river in Vietnamese Mekong Delta. *Journal of Japan Society of Civil Engineers, Series B1 (Hydraulic Engineering)*, 74, 871–876.

Binh, D. V., Kantoush, S., Sumi, T., & Mai, N. P. (2018). Impact of Lancang cascade dams on flow regimes of Vietnamese Mekong Delta. *Annual Journal of Hydraulics Engineering*, 74, 487–492.

Binh, D. V., Kantoush, S., & Sumi, T. (2020). Changes to long-term discharge and sediment loads in the Vietnamese Mekong Delta caused by upstream dams. *Geomorphology*, 353, 107011.

Bizzi, S., Dinh, Q, Bernardi, D., Schippa, L., & Soncini-Sessa, R. (2015). On the control of riverbed incision induced by run-of-river power plant. *Water Resources Research*, 51(7), 5023–5040.

Bravard, J.-P., Goichot, M., & Gaillot, S. (2013). Geography of sand and gravel mining in the lower Mekong River: First survey and impact assessment. *EchoGéo*, 26, 1–18.

Bravard, J.-P., Goichot, M., & Tronchère, H. (2014). An assessment of sediment-transport processes in the lower Mekong River based on deposit grain sizes, the CM technique and flow-energy data. *Geomorphology*, 207, 174–189.

Brunier, G., Anthony, E. J., Goichot, M., Provansal, M., & Dussouillez, P. (2014). Recent morphological changes in the Mekong and Bassac River channels, Mekong Delta: The marked impact of river-bed mining and implications for delta destabilisation. *Geomorphology*, 224, 177–191.

Chapman, A., & Darby, S. (2016). Evaluating sustainable adaptation strategies for vulnerable mega-deltas using system dynamics modelling: Rice agriculture in the Mekong Delta's an Giang Province, Vietnam. *Science of the Total Environment*, 559, 326–338.

Dang, T. D., Cochrane, T. A., Arias, M. E., Van, P. D. T., & Vries, T. T. D. (2016). Hydrological alterations from water infrastructure development in the Mekong floodplains. *Hydrological Processes*, 30, 3824–3838.

Darby, S. E., Hackey, C. R., Leyland, J., Kummu, M., Lauri, H., Parsons, D. R., Best, J. L., Nicholas, A. P., & Aalto, R. (2016). Fluvial

sediment supply to a mega-delta reduced by shifting tropical-cyclone activity. *Nature*, 539, 276–279.

Darby, S. E., Leyland, J., Kummu, M., & Timo, A. R. (2013). Decoding the drivers of bank erosion on the Mekong River: The roles of the Asian monsoon, tropical storms, and snowmelt. *Water Resources Research*, 49, 2146–2163.

Delgado, J. M., Apel, H., & Merz, B. (2010). Flood trends and variability in the Mekong River. *Hydrology and Earth System Sciences*, 14(3), 407–418.

England, J. F., Cohn, T. A., Faber, B. A., Stedinger, J. R., Thomas, W. O., Veilleuz, A. G., Kiang, J. E., & Mason, R. R. (2018). Guidelines for determining flood flow frequency – Bulletin 17C (ver. 1.1, May 2019): U.S. Geological Survey Techniques and Methods, book 4, chap. B5, 148.

Eslami, S., Hoekstra, P., Trung, N. N., Kantoush, S. A., Binh, D. V., Dung, D. D., Quang, T. T., & Vegt, M. V. D. (2019). Tidal amplification and salt intrusion in the Mekong Delta driven by anthropoginic sediment starvation. *Scientific Reports*, 9, 18746.

Fan, H., He, D., & Wang, H. (2015). Environmental consequences of damming the mainstream Lancang-Mekong River: A review. *Earth Science Reviews*, 146(2), 77–91.

Fitzhugh, T. W., & Vogel, R. M. (2011). The impact of dams on flood flows in the United States. *River Research and Applications*, 27(10), 1192–1215.

Foreman, M. G. G., Crawford, W. R., & Marsden, R. F. (1995). De-tiding: Theory and practices. *Coastal and Estuarine Studies*, 47, 203–239.

Gugliotta, M., Saito, Y., Nguyen, V. L., Ta, T. K. O., Nakashima, R., Tamura, T., Uehara, K., Katsuki, K., & Yamamoto, S. (2017). Process regime, salinity, morphological and sedimentary trends along the fluvial marine transition zone of the mixed-energy Mekong River Delta, Vietnam. *Continental Shelf Research*, 147, 7–26.

Ha, D. T., Ouillon, S., & Vinh, G. V. (2018). Water and suspended sediment budgets in the lower Mekong from high-frequency measurements (2009-2016). *Water*, 10, 846.

Hackney, C. R., Darby, S. E., Parsons, D. R., Leyland, J., Best, J. L., Aalto, R., Nicholas, A. P., & Houseago, R. C. (2020). River bank instability from unsustainable sand mining in the lower Mekong River. *Nature Sustainability*, 3, 217–225.

Haddeland, I., Lettenmaier, D. P., & Skaugen, T. (2006). Effects of irrigation on the water and energy balances of the Colorado and Mekong River basins. *Journal of Hydrology*, 324, 210–223.

Hoa, L. T. V., Nhan, N. H., Wolanski, E., Cong, T. T., & Shigeko, H. (2007). The combined impact on the flooding in Vietnam's Mekong River delta of local man-made structures, sea level rise, and dams upstream in the river catchment. *Estuarine, Coastal and Shelf Science*, 71, 110–116.

Hoang, L. P., Lauri, H., Kummu, M., Koponen, J., van Vliet, M. T. H., Supit, I., Leemans, R., Kabat, P., & Ludwig, F. (2016). Mekong River flow and hydrological extremes under climate change. *Hydrology and Earth System Sciences*, 20, 3027–3041.

Hoang, L. P., van Vliet, M. T. H., Kummu, M., Lauri, H., Koponen, J., Supit, I., Leemans, R., Kabat, P., & Ludwig, F. (2019). The Mekong's future flows under multiple drivers: How climate change, hydropower developments and irrigation expansions drive hydrological changes. *Science of the Total Environment*, 649, 601–609.

Hoanh, C. T., Jirayoot, K., Lacomne, G., & Srunetr, V. (2010). Impacts of climate change and development on Mekong flow regimes First assessment – 2009. MRC Management Information Booklet Series No. 4, Mekong River Commission, Vientiane, Lao PDR.

Ijaz, M. W., Mahar, R. B., Ansari, K., Siyal, A. A., & Anjum, M. N. (2020). Integrated assessment of contemporary hydro-geomorphologic evolution of the Indus River estuary, Pakistan in context to regulated fluvial regimes. *Estuarine, Coastal and Shelf Science*, 236, 106657.

Jordan, C., Tiede, J., Lojek, O., Visscher, J., Apel, H., Nguyen, H. Q., Quang, C. N. X., & Schlurmann, T. (2019). Sand mining in the Mekong Delta revisited - current scales of local sediment deficits. *Scientific Reports*, 9, 17823.

Kantoush, S., Binh, D. V., Sumi, T., & Trung, L. V. (2017). Impact of upstream hydropower dams and climate change on hydrodynamics of Vietnamese Mekong Delta. *Journal of Japan Society of Civil Engineers, Series B1 (Hydraulic Engineering)*, 73(4), I_109–I_114.

Kendall, A. M. G. (1938). A new measure of rank correlation. *Oxford Journal*, 30, 81–93.

Koehnken, L. (2014). Discharge sediment monitoring project (DSMP) 2009–2013 Summary & Analysis of results. Final Report. Mekong River Commission/Gesellschaft für Internationale Zusammenarbeit, Phnom Penh, Cambodia.

Kondolf, G. M., Rubin, Z. K., & Minear, J. T. (2014). Dams on the Mekong: Cumulative sediment starvation. *Water Resources Research*, 50, 5158–5169.

Kummu, M., Lu, X. X., Rasphone, A., Sarkkula, J., & Koponen, J. (2008). Riverbank changes along the Mekong River: Remote sensing detection in the Vientiane–Nong Khai area. *Quaternary International*, 186, 100–112.

Kummu, M., Lu, X. X., Wang, J. J., & Varis, O. (2010). Basin-wide sediment trapping efficiency of emerging reservoirs along the Mekong. *Geomorphology*, 119, 181–197.

Kummu, M., & Varis, O. (2007). Sediment-related impacts due to upstream reservoir trapping, the lower Mekong River. *Geomorphology*, 85, 275–293.

Lauri, H., De-Moel, H., Ward, P. J., Räsänen, T. A., Keskinen, M., & Kummu, M. (2012). Future changes in Mekong River hydrology: Impact of climate change and reservoir operation on discharge. *Hydrology and Earth System Sciences*, 16(12), 4603–4619.

Li, D., Long, D., Zhao, J., Lu, H., & Hong, Y. (2017). Observed changes in flow regimes in the Mekong River basin. *Journal of Hydrology*, 551, 217–232.

Li, J., Dong, S., Yang, Z., Peng, M., Liu, S., & Li, X. (2012). Effects of cascade hydropower dams on the structure and distribution of riparian and upland vegetation along the middle-lower Lancang-Mekong River. *Forest Ecology and Management*, 284, 251–259.

Lu, X. X., Kummu, M., & Oeurng, C. (2014). Reappraisal of sediment dynamics in the lower Mekong River, Cambodia. *Earth Surface Processes and Landforms*, 39, 1855–1865.

Lu, X. X., Li, S., Kummu, M., Padawangi, R., & Wang, J. J. (2014). Observed changes in the water flow at Chiang Saen in the lower Mekong: Impacts of Chinese dams? *Quaternary International*, 336, 145–157.

Lu, X. X., & Siew, R. Y. (2006). Water discharge and sediment flux changes over the past decades in the lower Mekong River: Possible impacts of the Chinese dams. *Hydrology and Earth System Sciences*, 10, 181–195.

Mai, N. P., Kantoush, S., Sumi, T., Thang, T. D., Trung, L. V., & Binh, D. V. (2018). Assessing and adapting the impacts of dams operation and sea level rising on saltwater intrusion into the Vietnamese Mekong Delta. *Journal of Japan Society of Civil Engineers, Series B1 (Hydraulic Engineering)*, 74, 373–378.

Manh, N. V., Dung, N. V., Hung, N. N., Kummu, M., Merz, B., & Apel, H. (2015). Future sediment dynamics in the Mekong Delta floodplains: Impacts of hydropower development, climate change and sea level rise. *Global and Planetary Change*, 127, 22–33.

Manh, N. V., Dung, N. V., Hung, N. N., Merz, B., & Apel, H. (2014). Large-scale suspended sediment transport and sediment deposition in the Mekong Delta. *Hydrology and Earth System Sciences*, 18, 3033–3053.

Mann, H. B. (1945). Nonparametric tests against trend. *Econometrica*, 13, 245–259.

Park, E., Ho, H. L., Tran, D. D., Yang, X., Alcantara, E., Merino, E., & Son, V. H. (2020). Dramatic decrease of flood frequency in the Mekong Delta due to river-bed mining and dyke construction. *Science of the Total Environment*, 723, 138066.

Pettitt, A. N. (1979). A non-parametric approach to the change-point problem. *Applied Statistics*, 28(2), 126–135.

Räsänen, T. A., Someth, P., Lauri, H., Koponen, J., Sarkkula, J., & Kummu, M. (2017). Observed river discharge changes due to hydropower operations in the upper Mekong basin. *Journal of Hydrology*, 545, 28–41.

Richter, B. D., Baumgartner, J. V., Braun, D. P., & Powell, J. (1998). A spatial assessment of hydrologic alteration within a river network. *Regulated Rivers: Research & Management*, 14, 329–340.

Rubin, Z. K., Kondolf, G. M., & Carling, P. A. (2015). Anticipated geomorphic impacts from Mekong basin dam construction. *International Journal of River Basin Management*, 13(1), 105–121.

Sen, P. K. (1968). Estimates of the regression coefficient based on Kandall's tau. *Journal of the American Statistical Association*, 63, 1379–1389.

Tran, D. D., Halsema, G. V., Hellegers, P. J. G. J., Hoang, L. P., & Ludwig, F. (2019). Long-term sustainability of the Vietnamese Mekong Delta in question: An economic assessment of water management alternatives. *Agricultural Water Management*, 223, 105703.

Tran, D. D., Halsema, G. V., Hellegers, P. J. G. J., Ludwig, F., & Wyatt, A. (2018). Questioning tripple rice intensification on the Vietnamese Mekong Delta floodplains: An environmental and economic analysis of current land-use trends and alternatives. *Journal of Environmental Management*, 217, 429–441.

Triet, N. V. K., Dung, N. V., Fujii, H., Kummu, M., Merz, B., & Apel, H. (2017). Has dyke development in the Vietnamese Mekong Delta shifted flood hazard downstream? *Hydrology and Earth System Sciences Discussion Review*, 21, 3991–4010.

Vogel, R. M., Sieber, J., Archfield, S. A., Smith, M. P., Apse, C. D., & Huber-Lee, A. (2007). Relations among storage, yield, and instream flow. *Water Resources Research*, 43, W05403.

Wang, J. J., Lu, X. X., & Kummu, M. (2011). Sediment load estimates and variations in the lower Mekong River. *River Research and Applications*, 27, 33–46.

Xue, Z., Liu, J. P., & Ge, Q. (2011). Changes in hydrology and sediment delivery of the Mekong River in the last 50 years: Connection to damming, monsoon, and ENSO. *Earth Surface Processes and Landforms*, 36, 296–308.

Yang, D., Ye, B., & Kane, D. (2004). Streamflow changes over Siberian Yenisei River basin. *Journal of Hydrology*, 296, 59–80.

Yu, M., Li, Q., Lu, G., Cai, T., Xie, W., & Bai, X. (2013). Investigation into the impacts of the Gezhouba and the three gorges reservoirs on the flow regime of the Yangtze River. *Journal of Hydrologic Engineering*, 18(9), 1098–1106.

Zhang, Q., Singh, V. P., & Li, K. (2014). Trend, periodicity and abrupt change in streamflow of the East River, the Pearl River basin. *Hydrological Processes*, 28(2), 305–314.

SUPPORTING INFORMATION

Additional supporting information may be found online in the Supporting Information section at the end of this article.